ฟรีเดลคราฟต์แอซิเลชันของสารประกอบแอโรแมติกบนอะลูมิเนียมออกไซด์พิลลาร์เคลย์อิมเพรกเนตด้วยอินเดียมคลอไรด์

นางสาวอุทุมพร เลิศวิไล

ศูนย์วิทยทรัพยากร
จุฬาลงกรณ์มหาวิทยาลัย

วิทยานิพนธ์นี้เป็นส่วนหนึ่งของการศึกษาตามหลักสูตรปริญญาวิทยาศาสตรมหาบัณฑิต
สาขาวิชาปิโตรเคมีและวิทยาศาสตร์พอลิเมอร์
คณะวิทยาศาสตร์ จุฬาลงกรณ์มหาวิทยาลัย
ปีการศึกษา 2552
ลิขสิทธิ์ของจุฬาลงกรณ์มหาวิทยาลัย

FRIEDEL-CRAFTS ACYLATION OF AROMATIC COMPOUNDS OVER $InCl_3$-IMPREGNATED ALUMINIUM OXIDE-PILLARED CLAY

Miss Autumporn Lertwilai

ศูนย์วิทยทรัพยากร
จุฬาลงกรณ์มหาวิทยาลัย

A Thesis Submitted in Partial Fulfillment of the Requirements
for the Degree of Master of Science Program in Petrochemistry and Polymer Science
Faculty of Science
Chulalongkorn University
Academic Year 2009
Copyright of Chulalongkorn University

Thesis Title	FRIEDEL-CRAFTS ACYLATION OF AROMATIC COMPOUNDS OVER $InCl_3$-IMPREGNATED ALUMINIUM OXIDE-PILLARED CLAY
By	Miss Autumporn Lertwilai
Field of Study	Petrochemistry and Polymer Science
Thesis Advisor	Nipaka Sukpirom, Ph.D.
Thesis Co-Advisor	Assistant Professor Warinthorn Chavasiri, Ph.D.

Accepted by the Faculty of Science, Chulalongkorn University in Partial Fulfillment of the Requirements for the Master's Degree

S. Hannongbua

.....Dean of the Faculty of Science

(Professor Supot Hannongbua, Dr. rer. nat.)

THESIS COMMITTEE

.....Chairman

(Professor Pattarapan Prasassarakich, Ph.D.)

Nipaka Sukpirom

.....Thesis Advisor

(Nipaka Sukpirom, Ph.D.)

Warinthorn Chavasiri

.....Thesis Co-Advisor

(Assistant Professor Warinthorn Chavasiri, Ph.D.)

W. Trakarnpruk

..... Examiner

(Associate Professor Wimonrat Trakarnpruk, Ph.D.)

Jinda Yeyongchaiwat

.....External Examiner

(Assistant Professor Jinda Yeyongchaiwat, Ph.D.)

อุทุมพร เลิศวิไล : ฟรีเดลคราฟต์แอซิเลชันของสารประกอบแอโรแมติกบนอะลูมิเนียมออกไซด์พิลลาร์เคลย์อิมเพรกเนตด้วยอินเดียมคลอไรด์ (FRIEDEL-CRAFTS ACYLATION OF AROMATIC COMPOUNDS OVER $InCl_3$-IMPREGNATED ALUMINIUM OXIDE-PILLARED CLAY) อ. ที่ปรึกษาวิทยานิพนธ์หลัก: อ. ดร. นิปกา สุขภิรมย์, อ. ที่ปรึกษาวิทยานิพนธ์ร่วม: ผศ. ดร. วรินทร ชวศิริ 64 หน้า

อะลูมิเนียมออกไซด์พิลลาร์แร่ดินเหนียวมอนต์มอริลโลไนต์ อิมเพรกเนตด้วยอินเดียมคลอไรด์ ($InCl_3$/Al-PLC) ถูกสังเคราะห์เพื่อใช้เร่งปฏิกิริยาฟรีเดลคราฟต์แอซิเลชันของแอนิโซลด้วยเบนโซอิลคลอไรด์ อะลูมิเนียมออกไซด์พิลลาร์เคลย์ (Al-PLC) ถูกเตรียมด้วยวิธีอินเทอร์คาเลชันและนำไปเผาที่ 500°C เป็นเวลา 1 ชั่วโมง จากนั้นอิมเพรกเนตด้วยอินเดียมไทรคลอไรด์ และนำไปเผาที่ 450°C เป็นเวลา 4 ชั่วโมง พิสูจน์โครงสร้างของ $InCl_3$/Al-PLC, Al-PLC และแร่ดินเหนียวมอนต์มอริลโลไนต์ ด้วยเทคนิคการเลี้ยวเบนของรังสีเอ็กซ์ การดูดซับแก๊สไนโตรเจน เอกซเรย์ฟลูออเรสเซนต์สเปกโทรสโกปี และอะตอมมิคแอดซอร์ฟชันสเปกโทรสโกปี ทดสอบความสามารถในการเร่งปฏิกิริยาของ $InCl_3$/Al-PLC เปรียบเทียบกับ Al-PLC และแร่ดินเหนียวมอนต์มอริลโลไนต์ พบว่า $InCl_3$/Al-PLC ให้ปริมาณผลิตภัณฑ์สูงกว่า Al-PLC ในขณะที่แร่ดินเหนียวมอนต์มอริลโลไนต์ไม่มีประสิทธิภาพในการเร่งปฏิกิริยานี้ ภาวะที่เหมาะสมสำหรับการผลิต 4-เมทอกซีเบนโซฟีโนนคือ อัตราส่วนโดยโมลของแอนิโซล ต่อเบนโซอิลคลอไรด์ เท่ากับ 1:3 และใช้ตัวเร่งปฏิกิริยา $InCl_3$/Al-PLC ที่มีปริมาณ $InCl_3$ เท่ากับ 0.03 มิลลิโมล ละลายใน 1,4-ไดออกเซน รีฟลักซ์เป็นเวลา 4 ชั่วโมง พบว่าให้ปริมาณผลิตภัณฑ์ 91% ภาวะที่เหมาะสมสำหรับการเกิดปฏิกิริยา สามารถนำไปประยุกต์กับสารแอโรแมติก และแอซิดคลอไรด์ชนิดอื่นๆ พบว่าให้ปริมาณผลิตภัณฑ์ในระดับปานกลางถึงสูง

สาขาวิชา ปิโตรเคมีและวิทยาศาสตร์พอลิเมอร์ ลายมือชื่อนิสิต อุทุมพร เลิศวิไล

ปีการศึกษา 2552 ลายมือชื่อ อ.ที่ปรึกษาหลัก นิปกา สุขภิรมย์

ลายมือชื่อ อ.ที่ปรึกษาร่วม

5072581523: MAJOR PETROCHEMISTRY AND POLYMER SCIENCE
KEYWORDS: INDIUM CHLORIDE / IMPREGNATE / PILLARED CLAY / ACYLATION

AUTUMPORN LERTWILAI: FRIEDEL-CRAFTS ACYLATION OF AROMATIC COMPOUNDS OVER $InCl_3$-IMPREGNATED ALUMINIUM OXIDE-PILLARED CLAY. THESIS ADVISOR: NIPAKA SUKPIROM, Ph.D., THESIS CO-ADVISOR: ASST. PROF. WARINTHORN CHAVASIRI, Ph.D., 64 pp.

$InCl_3$-impregnated aluminium oxide-pillared montmorillonite clay ($InCl_3$/Al-PLC) was synthesized in order to use as a catalyst for Friedel-Crafts acylation of anisole with benzoyl chloride. Aluminium oxide-pillared clay (Al-PLC) was prepared by the intercalation method and calcination at 500°C for 1 h. The impregnation with indium trichloride was done with calcination at 450°C for 4 h. $InCl_3$/Al-PLC, Al-PLC and montmorillonite clay were characterized using Powder X-ray Diffraction (XRD), N_2 adsorption-desorption, X-ray Fluorescence Spectrometry (XRF) and Inductively Coupled Plasma Optical Emission Spectrometry (ICP-OES) techniques. The catalytic activity of $InCl_3$/Al-PLC was compared with those of Al-PLC and montmorillonite. $InCl_3$/Al-PLC showed significantly higher yield than Al-PLC, and montmorillonite was not catalytic active in this reaction. The optimized condition for the production of 4-methoxybenzophenone was using the 1:3 mole ratio of anisole to benzoyl chloride and $InCl_3$/Al-PLC catalyst with the equivalent of 0.03 mmol $InCl_3$ in 1,4-dioxane. The reaction was carried out under reflux for 4 h, and gave an excellent yield of 91%. The optimized conditions could be applied to the Friedel-Crafts acylation of different aromatic compounds and acid chlorides with moderate to excellent yields.

Field of Study: Petrochemistry and Polymer science Student's Signature: Autumporn Lertwilai
Academic year: 2009 Advisor's Signature: Nipaka Sukpirom
Co-Advisor's Signature: W. Chavasiri

ACKNOWLEDGEMENTS

The author wishes to express her deep and sincere gratitude to her advisor Dr. Nipaka Sukpirom and Co-Advisor Assistant Professor Dr. Warinthorn Chavasiri, for their support and assistance. Their guidance helped her in all the time of research and writing of this thesis. The author also would like to express her gratitude to her thesis committee: Professor Dr. Pattarapan Prasassarakich, Associate Professor Dr. Wimonrat Trakarnpruk and Assistant Professor Dr. Jinda Yeyongchaiwat for their comments, corrections and suggestions as thesis examiners.

The author would like to thank Department of Chemistry and Program of Petrochemistry and Polymer Science, Faculty of Science, Chulalongkorn University and National Center of Excellent for Petroleum, Petrochemicals, and Advance Materials for the support of chemical and laboratory instrument.

The author would like to thank all members of Material Chemistry and Catalysis Research Unit and Natural Product Research unit for their assistance in her experiments and their kind suggestion. For all of my friends, thanks for their help and encouragement throughout the course of her research.

Finally, the author would like to thank her family for their love, understanding and always comfort.

ศูนย์วิทยทรัพยากร
จุฬาลงกรณ์มหาวิทยาลัย

CONTENTS

Pages

ABSTRACT (THAI) iv

ABSTRACT (ENGLISH) v

ACKNOWLEDGEMENTS vi

CONTENTS vii

LIST OF TABLES xi

LIST OF FIGURES xii

LIST OF SCHEMES xiii

LIST OF ABBREVIATIONS xiv

CHAPTER

I INTRODUCTION 1

1.1 Friedel-Crafts acylation 1

1.2 Literature reviews 2

1.2.1 Literature reviews of solid acid catalysts used in Friedel-Crafts acylation 2

1.2.2 Literature reviews of indium compound catalysts used in Friedel-Crafts reaction 3

1.2.3 Literature reviews of clay catalysts used in Friedel-Crafts reaction 5

1.3 Objectives 6

II THEORY 7

2.1 Clay 7

2.2 The structure of clay minerals 7

2.2.1 Basic unit 7

2.2.2 The combinations of basic sheets 8

2.3 Smectite clay 9

2.3.1 Montmorillonite clay 10

Pages

2.4 Properties of clay 10
2.4.1 Ion exchange 10
2.4.2 Swelling 11
2.4.3 Acidity of clays 12
2.5 Intercalation 12
2.6 Pillaring 13
2.7 Pillared clay 13
2.8 Impregnation 14
2.9 Characterization of clays and clay catalysts 14
2.9.1 Powder X-ray diffraction 14
2.9.2 Nitrogen adsorption-desorption isotherm 15
2.9.3 Inductively coupled plasma-atomic emission spectroscope (ICP-AES) 18
2.10 Friedel-Crafts acylation of aromatic compounds 19

III EXPERIMENTAL 20
3.1 Starting materials 20
3.1.1 Clays 20
3.1.2 Chemicals 20
3.2 Instrument, apparatus and analytical measurements 21
3.2.1 Centrifuge 21
3.2.2 Oven and furnace 21
3.2.3 X-ray diffractometer (XRD) 21
3.2.4 X-ray fluorescence spectroscopy (XRF) 22
3.2.5 Inductively coupled plasma spectroscopy (ICP) 22
3.2.6 Nitrogen adsorptometer 22
3.2.7 Nuclear magnetic resonance spectroscopy (NMR) 22
3.2.8 Chromatography 22
3.3 Homoionic clays 23
3.3.1 Purification of bentonite 23
3.3.2 Na-ion exchange 23

Pages

3.4 Synthesis of aluminium oxide-pillared clay (Al-PLC) 23
3.5 Synthesis of indium chloride impregnated aluminium oxide-pillared clay ($InCl_3$/Al-PLC) 24
3.6 Sample preparation for ICP 24
3.7 Optimum conditions study on Friedel-Crafts acylation of anisole with benzoyl chloride 24
3.7.1 General procedure 24
3.7.2 Effect of mole ratio of anisole to benzoyl chloride 25
3.7.3 Effect of the amount of catalyst 25
3.7.4 Effect of reaction time 25
3.7.5 Effect of type of organic solvents 25
3.8 The screening of substrates 25
3.8.1 Variation of aromatic compounds 25
3.8.2 Variation of acid chlorides 25
3.9 Reuse of catalyst 26

IV RESULTS AND DISCUSSION 27
4.1 The characterization of clays 27
4.1.1 The characterization of raw bentonite 27
4.2 The synthesis and characterization of homoionic clay 28
4.2.1 The purification of bentonite 28
4.2.2 Na-ion exchange of montmorillonite 29
4.3 The characterization of aluminium oxide-pillared clay (Al-PLC) 30
4.4 The characterization of indium chloride impregnated aluminium oxide-pillared clay ($InCl_3$/Al-PLC) 31
4.5 Determination of indium and chloride contents 33
4.6 Nitrogen adsorption/desorption (BET) 33
4.7 Catalytic activity of Al-PLC and $InCl_3$/Al-PLC in Friedel-Crafts acylation 34

Pages

4.7.1 Activity of montmorillonite, Al-PLC and $InCl_3$/Al-PLC catalysts in Friedel-Crafts acylation of anisole with benzoyl chloride 34
4.7.2 Study on the optimum condition for Friedel-Crafts acylation of anisole with benzoyl chloride by $InCl_3$/Al-PLC 37
4.7.2.1 Effect of the mole ratio of anisole to benzoyl chloride 37
4.7.2.2 Effect of the amount of catalyst 38
4.7.2.3 Effect of the reaction time 39
4.7.2.4 Effect of the type of organic solvents 39
4.7.3 The screening of substrates 40
4.7.3.1 Type of aromatic compounds 41
4.7.3.2 Type of acid chlorides 42
4.8 Regenerated catalysts 45
4.8.1 The characterization of the regenerated catalyst by XRD 45
4.8.2 Activity of regenerated $InCl_3$/Al-PLC in Friedel-Crafts acylation of anisole with benzoyl chloride 46

V CONCLUSION 47

REFERENCES 49
APPENDICES 53
VITAE 64

LIST OF TABLES

Tables **Pages**

2.1 Features of adsorption isotherms 16
2.2 IUPAC classification of pores 17
3.1 Bentonite compositions 20
4.1 The indium and chloride contents in clays sample 33
4.2 BET specific surface area 34
4.3 Activities of various catalysts in Friedel-Crafts acylation 35
4.4 Effect of mole ratio of anisole to benzoyl chloride 37
4.5 Effect of the amount of $InCl_3$ in $InCl_3$/Al-PLC 38
4.6 Effect of type of organic solvents 40
4.7 Synthesis of aromatic ketones from various aromatic compounds under the optimal condition 41
4.8 Synthesis of aromatic ketones from various acid chlorides under the optimal condition 42
4.9 Products obtained from various aromatic compounds and acid chlorides 43
4.10 Indium chloride content and BET specific surface area of regenerated $InCl_3$/Al-PLC and $InCl_3$/Al-PLC 45
4.11 Activity of regenerated $InCl_3$/Al-PLC 46

ศูนย์วิทยทรัพยากร
จุฬาลงกรณ์มหาวิทยาลัย

LIST OF FIGURES

Figures **Pages**

2.1 A single tetrahedral silica (a) and a sheet structure of silica tetrahedral arranged in a hexagonal network (b) 8

2.2 A single octahedral unit (a) and a sheet structure of octahedral unit arranged in a hexagonal network (b) 8

2.3 Structure of 1:1 layer type (T = Tetrahedral sheet and O = Octahedral sheet) 9

2.4 Structure 2:1 layer type, T:O:T clay (b) (T = Tetrahedral sheet and Octahedral sheet) 9

2.5 Structure of smectite clay 10

2.6 Diffraction of X-ray by regular planes of atoms 15

2.7 The IUPAC classification of adsorption isotherms 16

2.8 A typical plasma source 18

4.1 XRD pattern of raw bentonite 28

4.2 XRD patterns of (a) raw bentonite and (b) montmorillonite 29

4.3 XRD patterns of (a) montmorillonite and (b) Na-montmorillonite 30

4.4 XRD patterns of (a) Na-montmorillonite and (b) aluminium oxide-pillared clay (Al-PLC) 31

4.5 XRD patterns of (a) aluminium oxide-pillared clay (Al-PLC) and (b) indium chloride impregnated aluminium oxide-pillared clay ($InCl_3$/Al-PLC) 32

4.6 Simulation of XRD patterns of indium trichloride ($InCl_3$) from database JCPDS: 34-1145 32

4.7 Effect of reaction time on the percent yield of 4-MBP 39

4.8 XRD patterns of (a) regenerated $InCl_3$/Al-PLC and (b) $InCl_3$/Al-PLC 45

LIST OF SCHEMES

Schemes **Pages**

2.1 The exchange properties of cations with clays 11
2.2 Diagram for the preparation of pillared clay compounds (cross section) 13
2.3 Diagram for the preparation of impregnated pillared clay (cross section) 14
2.4 Acylation of benzene with benzoyl chloride 19
4.1 Mechanism of Friedel-Crafts acylation of aromatic compounds on $InCl_3$/Al-PLC 36

ศูนย์วิทยทรัพยากร
จุฬาลงกรณ์มหาวิทยาลัย

LIST OF ABBREVIATIONS

BET	Brunauer-Emmett-Teller
δ	chemical shift
J	coupling constant (NMR)
°C	degree Celsius
$CDCl_3$	deuterated chloroform
d	doublet (NMR)
g	gram (s)
Hz	hertz
h	hour (s)
ICP-OES	inductively couple plasma optical emission spectrometry
Kg	kilogram
mL	milliliter (s)
mmol	millimole (s)
min	minute (s)
M	molar
m	multiplet (NMR)
NMR	Nuclear magnetic resonance
q	quartet (NMR)
Å	Angstrom unit
CEC	cation exchange capacity
rt	room temperature
s	singlet (NMR)
t	triplet (NMR)
XRD	X-ray diffraction
4-MBP	4-methoxybenzophenone

ศูนย์วิทยทรัพยากร
จุฬาลงกรณ์มหาวิทยาลัย

CHAPTER I

INTRODUCTION

1.1 Friedel-Crafts acylation

Aromatic ketones are important fine chemicals and exploited intermediates for the production of fine chemicals in cosmetics, pharmaceuticals, colorants, agrochemicals and other chemical industries. The common method for the synthesis of aromatic ketones is the homogeneous Friedel-Crafts acylation of aromatic compounds with acid chlorides using Lewis acid (such as $AlCl_3$, $FeCl_3$ and $SnCl_4$) as a catalyst; however, using this type of catalyst possesses several problems, such as highly moisture sensitivity, difficulty during separation, severe corrosion and high toxicity. The catalysts preferably used in industrial processes should be clean towards environment, reusable, noncorrosive and cheap. Thus the search for solid acid catalysts in order to replace corrosive Lewis acid catalysts is essential. The solid acid catalysts such as zeolites [1], heteropoly acids [2], sulfated zirconia [3] and clay minerals [4] have been reported on their catalytic efficiencies for Friedel-Crafts acylation.

In this work, clay minerals were chosen as the support because it is naturally abundant, environmentally safe, and very cheap solid. It has been reported that clays could act as a catalyst in Friedel-Crafts acylation but giving a low efficiency [3]. Therefore, clays would be modified by the pillaring of aluminium oxide between clay layers in order to increase the surface area and allow the easy access of substrates and by the impregnation of indium trichloride in order to increase the catalytic activity.

The aim of this research is to synthesize $InCl_3$-impregnated aluminium oxide-pillared clay ($InCl_3$/Al-PLC) and aluminium oxide-pillared clay (Al-PLC). All catalysts were tested for their catalytic activities in the Friedel-Crafts acylation of aromatic compounds.

1.2 Literature reviews

1.2.1 Literature reviews of solid acid catalysts used in Friedel-Crafts acylation

In 1998, Quaschning *et al.* [5] studied the catalytic activity in Friedel-Crafts acylation of anisole with benzoyl chloride and benzoic anhydride using ammonium sulfate modified zirconia ($ZR/amSO_4$) catalyst. The catalyst showed high conversion of both benzoyl chloride (76%) and benzoic anhydride (80%).

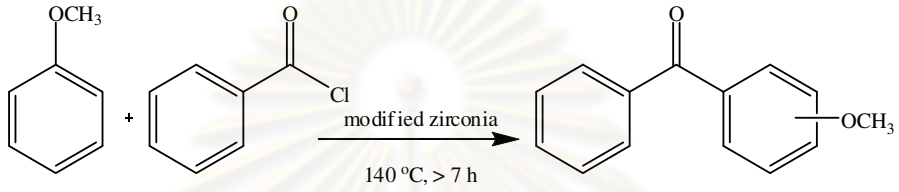

In 2005, Bing *et al.* [6] studied the catalytic activity of zeolites for Friedel-Crafts acylation of anisole with benzoyl chloride. H-Beta zeolite showed higher activity than the other zeolites. The conversion of benzoyl chloride was 99.5% and the selectivity for 4-methoxybenzophenone was 91.2%.

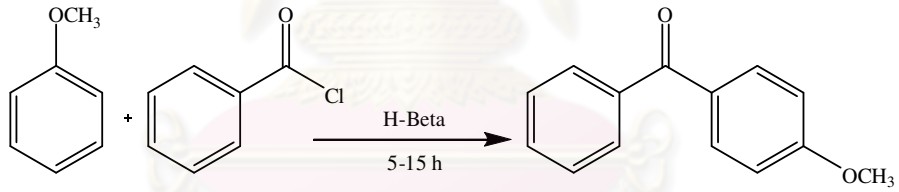

In 2003, Yadav *et al.* [3] synthesized the Cs substituted heteropolyacid supported on K-10 clay ($Cs_{2.5}H_{0.5}PW_{12}O_{40}$/K-10). The catalytic activity was tested for Friedel-Crafts acylation of anisole with benzoyl chloride, resulting to 37% conversion for the production of 4-methoxybenzophenone.

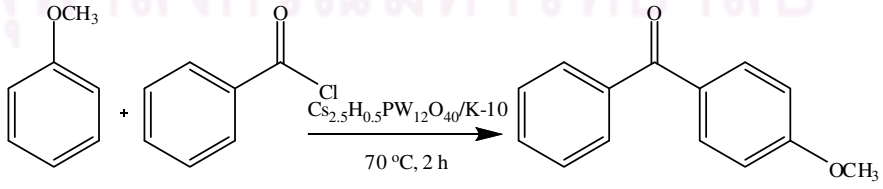

In 2008, Yadav *et al.* [7] studied the Friedel-Crafts acylation of 1,3-dibenzyloxybenzene with acetic anhydride using several solid acids. The catalytic result of $Cs_{2.5}H_{0.5}PW_{12}O_{40}$/K-10 showed the highest selectivity and the catalyst could

be reused for several times. The selectivity to 3,5-dibenzyloxyacetophenone of the catalysts was in the order of $Cs_{2.5}H_{0.5}PW_{12}O_{40}$/K-10 > Indion-130 (ion exchange resin) > sulfated zirconia > Amberlyst-36 (acidic ion exchange resin) > UDCaT-5 (modified zirconia).

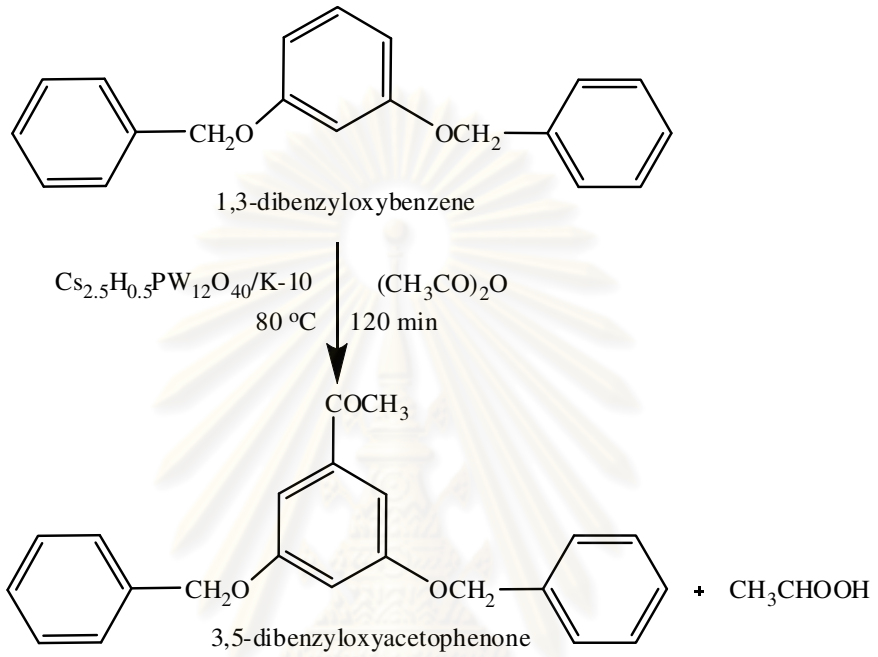

1.2.2 Literature reviews of indium compound catalysts used in Friedel-Crafts reaction

Choudhary *et al.* have studied Friedel-Crafts reaction using both metal oxides and metal chlorides. In 2000, the group synthesized Ga_2O_3 and In_2O_3 supported on Si-MCM-41 (Ga_2O_3/Si-MCM-41 and In_2O_3/Si-MCM-41) by impregnation method. The catalysts were used in Friedel-Crafts acylation of toluene with benzoyl chloride. It was found that, at 83% conversion, In_2O_3 catalyst used the reaction period of 2.47 h, which is less time than 3.42 h when Ga_2O_3 catalyst was used [8].

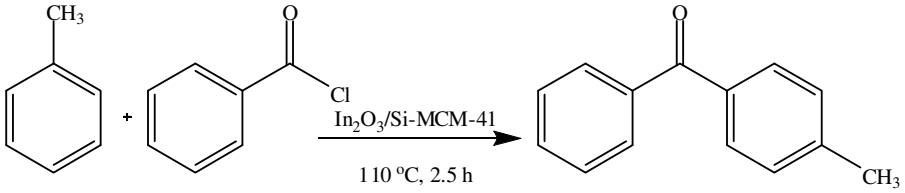

In 2002, the In_2O_3/Si-MCM-41 was tested for its catalytic activity towards Friedel-Crafts acylation of benzene and substituted benzenes with benzoyl chloride. The reaction period needed for different aromatics were increased as anisole < mesitylene < p-xylene < toluene < benzene [9].

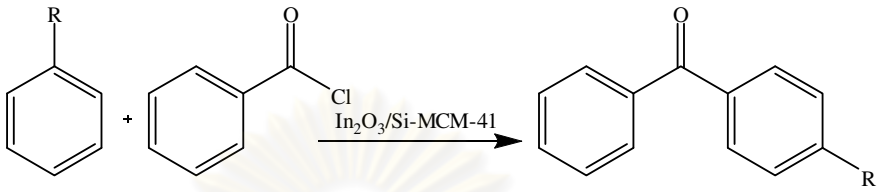

In 2003, the same group tested the catalytic activity in Friedel-Crafts acylation of aromatic compounds (benzene, toluene, p-xylene and anisole) over In_2O_3 supported on H-Beta zeolite. The catalyst was synthesized by impregnation method. This catalyst showed higher conversion (80%) than pure H-Beta zeolite (30%) [10].

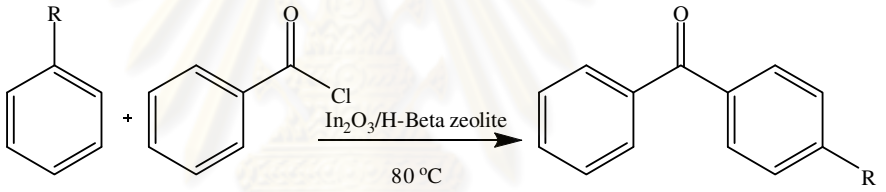

In 2000, Choudhary *et al.* synthesized metal chlorides impregnated on montmorillonite K-10 and Si-MCM-41 and tested the catalytic activities in Friedel-Crafts alkylation of benzene with benzyl chloride. The support showed the reaction period in the order of Si-MCM-41 > montmorillonite K-10. The metals chloride supported catalysts showed the activity in the order of $InCl_3$ > $GaCl_3$ >> $AlCl_3$, as supported on montmorillonite K-10 [11].

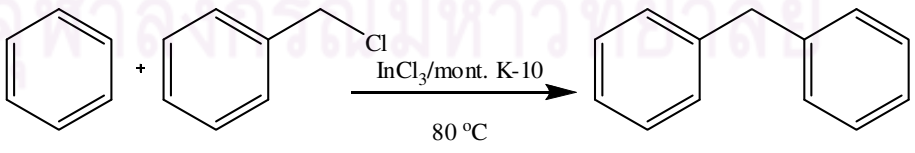

In 2001, they studied the catalytic activity in Friedel-Crafts acylation of benzene with acyl chlorides (benzoyl chloride, butyryl chloride and phenyl acetyl chloride) using various catalysts such as $InCl_3$, $GaCl_3$ and $ZnCl_2$ supported on clays (montmorillonite-K10, montmorillonite-KSF and kaolin). The catalysts were synthesized by an

impregnation method. The $InCl_3$ supported catalysts showed highest activity of 80% conversion and montmorillonite-K10 was the best support. The metals chloride supported on the same support catalysts showed the activity in the order of $InCl_3$ > $GaCl_3$ >> $ZnCl_2$. The support showed the activity in the order of montmorillonite-K10 > montmorillonite-KSF >> kaolin [12].

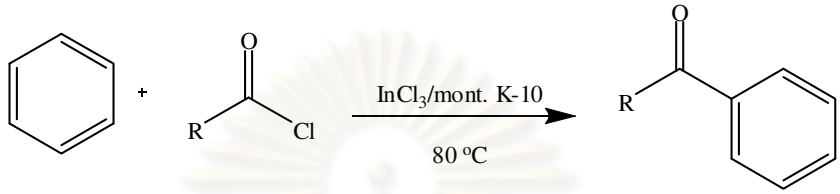

In 2002, the $InCl_3$/Si-MCM-41 was used in Friedel-Crafts acylation of aromatic compounds (benzene, toluene, p-xylene, mesitylene, anisole, naphthalene, 2-methylnaphthalen and 2-methoxynaphthalen) with benzoyl chloride. $InCl_3$/Si-MCM-41 showed high activity of 60-88% yield. The acylation activity attributed to the redox property of the catalyst ($E^0_{In^{3+}/In^{1+}}$ = -0.44V), indicating the redox mechanism of the reaction [13].

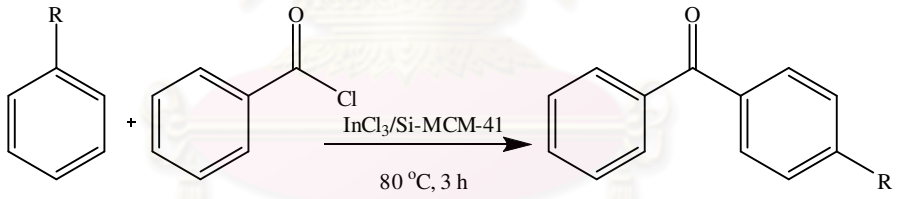

1.2.3 Literature reviews of clay catalysts used in Friedel-Crafts reaction

In 1990, Cornelis *et al.* [4] tested the catalytic activity of metals chloride (Al^{3+}, Co^{2+}, Cr^{3+}, Cu^{2+}, Fe^{3+}, Ti^{4+}, Zn^{2+}, Zr^{4+}) impregnated on montmorillonite K-10 supporter towards the Friedel-Crafts acylation of aromatic compounds (p-xylene, mesitylene and anisole) with benzoyl chloride. All catalysts showed high yields of the product, and the Fe^{3+} supported catalyst showed highest activity (98-100% yield) among these catalysts.

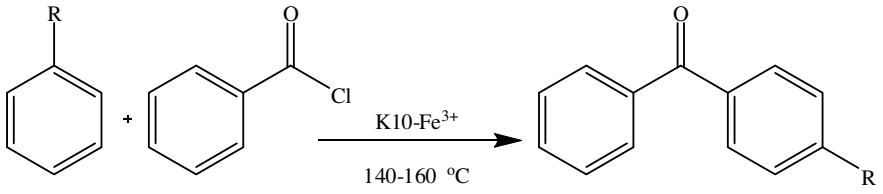

In 1999, Selvin *et al.* [14] synthesized the $ZnCl_2$ supported on montmorillonite (clayzic) and tested its catalytic activity in Friedel-Crafts acylation of anisole with acetic anhydride. The catalytic result showed 95-97% conversion for the production of 4-methoxyacetophenone.

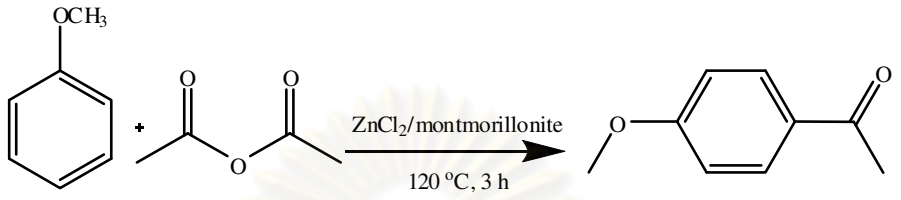

Although many heterogeneous catalysts for Friedel-Crafts acylation have been developed, but there was no report on the synthesis of $InCl_3$-impregnated aluminium oxide-pillared clay (In/Al-PLC) and its catalytic activity on Friedel-Crafts acylation of aromatic compounds.

1.3 Objectives

1. To synthesize $InCl_3$-impregnated aluminium oxide-pillared clay (In/Al-PLC) and aluminium oxide-pillared clay (Al-PLC).
2. To study on the optimum conditions for catalytic activity in Friedel-Crafts acylation of anisole with benzoyl chloride.
3. To investigate the catalytic activities in the Friedel-Crafts acylation of various aromatic compounds and acid chlorides.

ศูนย์วิทยทรัพยากร
จุฬาลงกรณ์มหาวิทยาลัย

CHAPTER II

THEORY

2.1 Clay

Clay minerals are crystalline hydrous aluminosilicates and classified as phyllosilicates or layer silicates. They are the most common products of water-rock interaction under earth-surface conditions. Clay minerals occur abundantly in nature. The properties of clays include high specific surface area, high sorptive capacity, reversible ion exchange and high acidity. Containing both Brønsted and Lewis acid types, clays have been exploited for various catalytic applications. Many organic reactions have been able to use clays as an efficient heterogeneous catalyst. Most importantly, clay catalysts have the advantage over homogeneous catalysts because of the very simple work up of the reaction mixture such as filtration or centrifugation [15].

2.2 The structure of clay minerals

Clay minerals possess a layered structure and their suspension in aqueous solution contains particles with the average diameter of about 2 μm [16]. Each clay layer is constructed from the combination of two basic types of layers: a sheet of corner-linked tetrahedral and a sheet of edge-linked octahedral. Normally, they are aluminum octahedral and silica tetrahedral sheets which are held together by sharing apical oxygen atoms [17].

2.2.1 Basic unit

2.2.1.1 Tetrahedral sheets

Tetrahedral sheet consists of tetrahedral units. Si^{4+} and Fe^{3+} are the dominant cations for tetrahedral sheets and each cation is surrounded with four oxygen atoms. The three corners of each tetrahedral share oxygen atoms with three other tetrahedral units to form hexagonal network. The apical oxygen points upward in the direction normal to the base of the sheet.

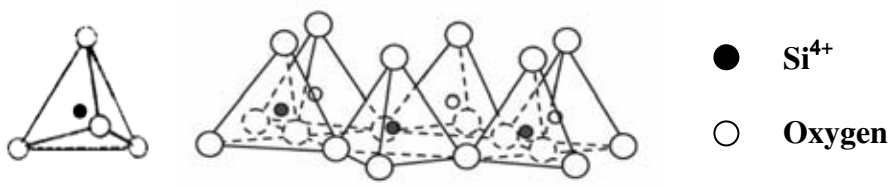

Figure 2.1 A single tetrahedral silica (a) and a sheet structure of silica tetrahedral arranged in a hexagonal network (b) [18].

2.2.1.2 Octahedral sheets

Octahedral sheet is constructed from the other octahedral units similar to the tetrahedral sheet. Each unit is containing the cation such as Al^{3+}or Mg^{2+} at the centre that is surrounded with six oxygen atoms. The neighboring octahedral units are connected in the edge-linked fashion and form the extended two dimensional structures.

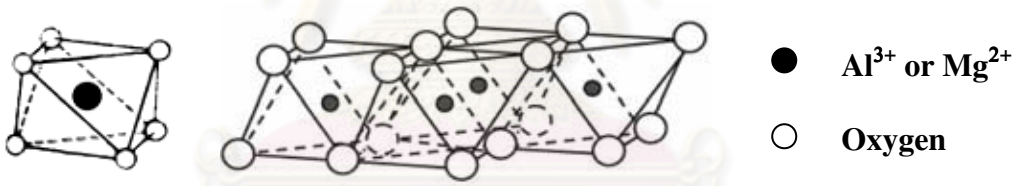

Figure 2.2 A single octahedral unit (a) and a sheet structure of octahedral unit arranged in a hexagonal network (b) [18].

2.2.2 The combinations of basic sheets

The combinations of basic sheets of clays could be divided into 2 types.

2.2.2.1 The 1:1 layer type (T:O)

Each layer of 1:1 type is consisted of one tetrahedral sheet (T) and one octahedral sheet (O). The apical oxygen atoms of a tetrahedral sheet point to the octahedral sheet and are shared with an octahedral sheet (O), such as kaolinite group.

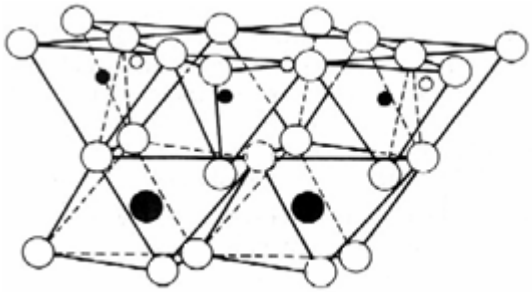

Figure 2.3 Structure of 1:1 layer type (T = Tetrahedral sheet and O = Octahedral sheet).

2.2.2.2 The 2:1 layer type (T:O:T)

A 2:1 layer is composed of two tetrahedral sheets and one octahedral sheet. This assembly makes a tetrahedral-octahedral-tetrahedral (T:O:T) sandwich layers such as smectite clay minerals. Bentonite, montmorillonite, and hectorite are the common smectite clay minerals.

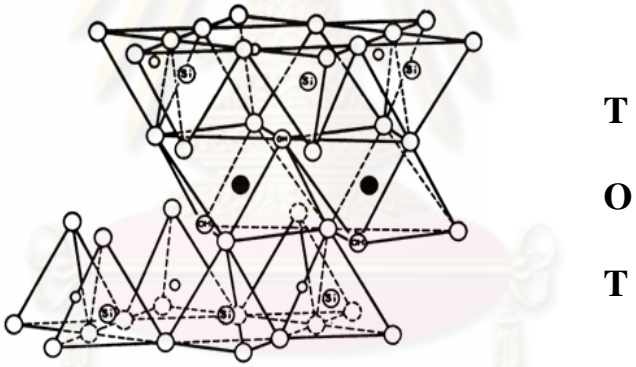

Figure 2.4 Structure 2:1 layer type, T:O:T clay (b) (T = Tetrahedral sheet and Octahedral sheet).

ศูนย์วิทยทรัพยากร
จุฬาลงกรณ์มหาวิทยาลัย

2.3 Smectite clay

The structures of smectite clays are derived from the mineral talc and pyrophyrite, which consist of a stacking of silica tetrahedral sheet ($Al_4Si_8O_{20}(OH)_4$) and alumina octahedral sheet ($Mg_6Si_8O_{20}(OH)_4$). The clay minerals of smectite group are composed of layers made up of two silica tetrahedral sheets with a central alumina octahedral sheet. Substitution of cations (for example, Al^{3+} for Si^{4+} in tetrahedral sheets and Mg^{2+} for Al^{3+} in octahedral sheets) either in tetrahedral or octahedral sheet

results in the formation of negative charge in the layers, which is balanced by additional cations located between the 2:1 layers. The repeating distance between the clay-layer is called the basal spacing, d_{001}. This value is easily identified by X-ray diffraction technique [19].

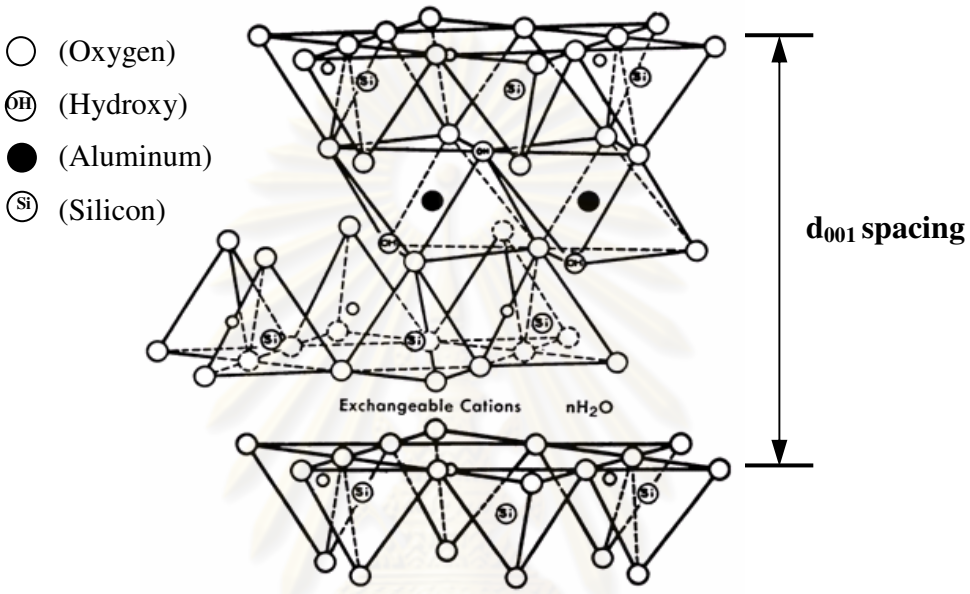

Figure 2.5 Structure of smectite clay.

2.3.1 Montmorillonite clay

Montmorillonite is the main constituent of bentonite (typically 80-90 wt %), the rest being a mixture of mineral impurities including quartz, crystobalite, feldspar and humic acids. Montmorillonite has an ideal formular of $(Si_8)(Al_{4-X}Mg_X)O_{20}(OH)_4A_X.nH_2O$ (where A is a monovalent or divalent cation), which Mg/Al in the octahedral sheet [20]. Montmorillonite is the most important smectite exploited in catalytic applications [21].

2.4 Properties of clay

2.4.1 Ion exchange

Clay minerals have the ability to adsorb and ion exchange. In general, the ideal neutral structure of clay minerals is disrupted by the introduction of charged imbalance. The two main sources of charged imbalance are: (1) the isomorphous

substitution of cations in the lattice by lower valent ions, such as the substitution of aluminum for silicon in the tetrahedral layer, magnesium for aluminum or sometimes lithium for magnesium in the octahedral layer, and (2) crystal defects. Leading to, the clay layers have an overall negative charge which is balanced by cations between the layers. These balance cations can be readily replaced by other cations in aqueous solution. In swelling clay minerals, such as smectites, the interlayer cations can be exchanged with cations from external solutions. It has been observed that the smaller the size and the higher the charge of the exchange cations, the more powerful that cations at replacing the interlayer exchangeable cations. The following series can be constructed [15].

$$M^{+} << M^{2+} < H_3O^{+} \sim K^{+} \sim NH^{4+} < M^{3+} < M^{4+}$$

$$\longrightarrow$$

Increasing exchange power

Scheme 2.1 The exchange properties of cations with clays.

The concentration of exchangeable cations (CEC) is usually measured in milliequivalents per 100 g of dried clay. Since smectites have relatively high concentration of interlayer cations, they have high cation exchange capacities (typically 70-120 meq/100 g) as well. Structural defects at layer edges give rise to an additional CEC and a small amount of anion exchange capacity [22].

2.4.2 Swelling

Many clay minerals adsorb water between their layers, which move the layers apart and cause the clay swelling. For efficient swelling, the released energy must be sufficient to overcome the attractive forces between the adjacent layers, such as lattice energy and hydrogen bonding from layer solvation. In aqueous solution, water forms strong hydrogen bonds with hydroxyl groups on hydrophilic octahedral layers, which allowing the swelling to occur for 1:1 clay minerals (kaolinite).

Similarly, the 2:1 clay minerals (smectite) also have the swelling ability, which depends on the solvation of interlayer cation and the layer charge. Clays with

2:1 structures and low layer charge have very low concentration of interlayer cations, therefore do not swell readily. At the other extreme, those with very high layer charges have strong electrostatic forces holding alternate anionic layers and the interlayer cations together, thus prevents the swelling. However, the 2:1 clays with univalent interlayer cations can swell most readily. For those with divalent, trivalent and polyvalent cations, swelling decrease accordingly. The extent of swelling can be observed by measuring interlayer separations using power X-ray diffraction [21, 22].

2.4.3 Acidity of clays

Acidity of clays is widely used as catalysts in organic reactions. Their acidic properties and catalytic activity depend on the exchanged cations. Clay minerals have both Brønsted and Lewis acid sites. The interlayer cations contribute to the acidity, with the Bronsted sites mainly associated with the interlamellar region. Some of these cations (e.g. Al^{3+}) dissociation their coordinated water molecule to produce acidic proton, which give Brønsted acidity. When the coordination of an organic compound to the cation, the cations is electron pair accepters and can ability act as Lewis acid catalyst [23]. In addition, clay minerals have layer surface and edge defects, which would result in weaker Brønsted and/or Lewis acidity, generally at low concentrations [15, 24].

2.5 Intercalation

Intercalation is the insertion of a guest species into the interlayer region of clay with the preservation of layered structure. Intercalation compound is proven by the XRD pattern, which must unambiguously show an increase in the spacing between adjacent layers, *i.e.* an increase in the basal spacing [17].

2.6 Pillaring

Pillaring is the process that used the intercalation procedure of compound into interlayer space, resulting to a pillared compound, which are thermally stable microporous and/or mesoporous materials with the preservation of a parent layer structure. A pillared derivative is distinguished from an ordinary intercalate by virtue of intracrystalline porosity made possible by the lateral separation of the intercalated guest [17].

2.7 Pillared clay

Pillared clays are materials obtained by the intercalation of guest molecules, which prepared by exchanged cations and polyoxocations into the interlayer of swellable clay, leading to the intercalated clays. Then the intercalated clays are calcined, the polyoxocations transform into metal oxide pillars, resulting to the pillared clay. The pillared clay has large specific surface area, acidity and good thermal stability, which is of great interest because of its potential application as catalysts and adsorbents in various fields.

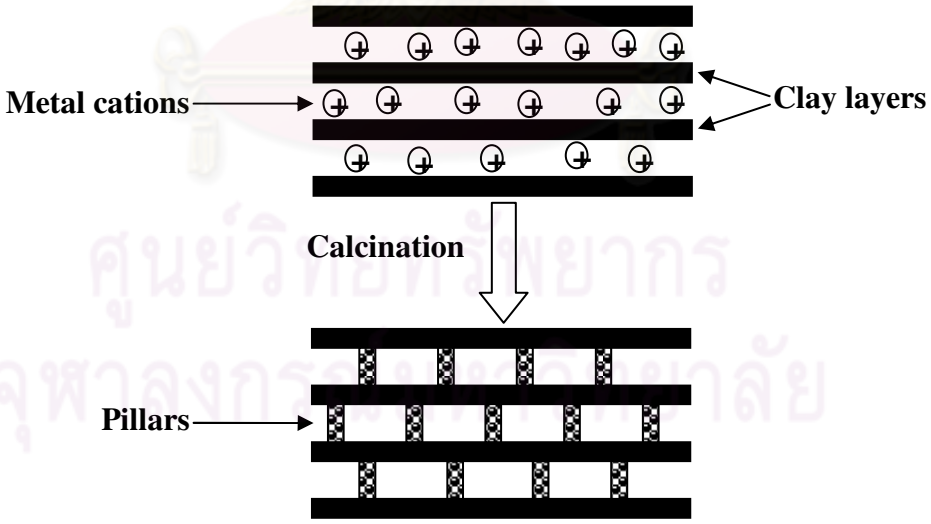

Scheme 2.2 Diagram for the preparation of pillared clay compounds (cross section).

2.8 Impregnation

Impregnation is the method for making a heterogeneous catalyst. Usually, a support or carrier is a porous material will be in contacted with a solution of compounds that little group are held onto the support. The impregnation method requires less equipment since the forming steps, filtering and washing are needless [25]. Scheme 2.3 shows the example of impregnation onto pillared clay.

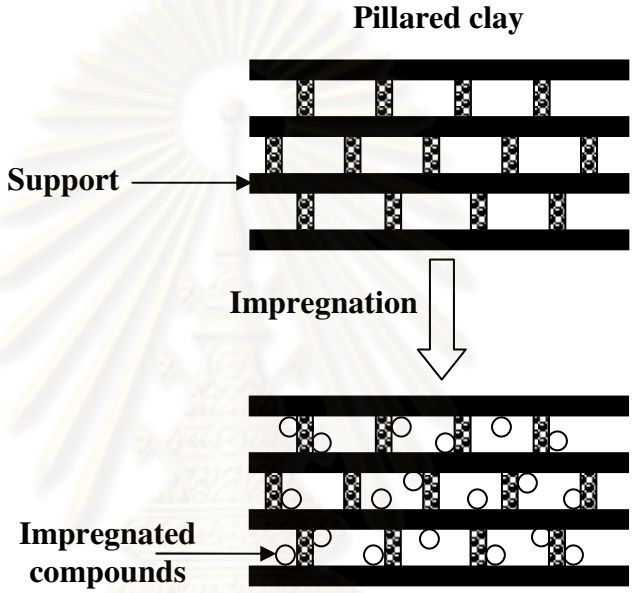

Scheme 2.3 Diagram for the preparation of impregnated pillared clay (cross section).

2.9 Characterization of clays and clay catalysts

2.9.1 Powder X-ray diffraction (XRD)

X-ray diffraction (XRD) is an instrumental technique for identification and characterization of crystalline materials. XRD is a technique which a collimated beam of monochromatic X-rays is directed onto the flat surface of a thin layer of finely ground material causing the X-rays is diffracted to specific angles. Fig. 2.7 shows a monochromatic beam of X-ray incident on the surface of crystal at an angle θ. The scattered intensity can be measured as a function of scattering angle 2θ [17]. An X-ray diffraction measurement the angle of incidence and detection are scanned. When the intensity of detected X-rays is plotted as a function of angle and X-ray diffraction pattern is obtained, which is characteristic for the sample material.

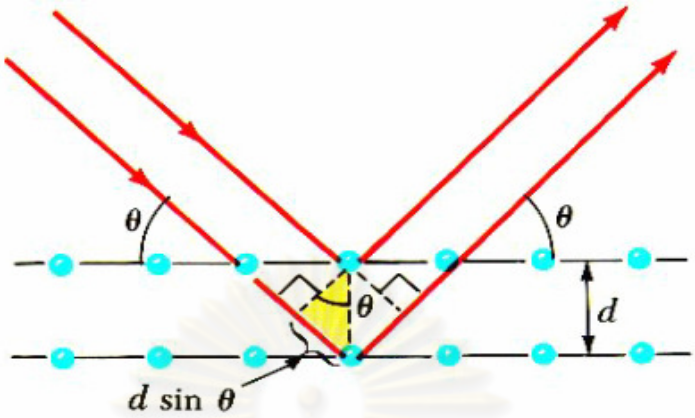

Figure 2.6 Diffraction of X-ray by regular planes of atoms [26].

Bragg diffraction is the general relationship between the wavelength of the incident x-rays, angle of incidence and spacing between the crystal lattice planes of atoms is known as the Bragg equation.

$$n\lambda = 2\ d\ \sin\theta$$

Where
- n = an integer of order of the diffracted beam
- λ = wavelength
- d = a distance between adjacent planes of atoms (d-spacing)
- θ = an angle between the incidence beam and the scattering planes

2.9.2 Nitrogen adsorption-desorption isotherm

The N_2 adsorption technique is used to determine the physical properties of material, such as the specific surface area, pore volume, pore diameter and pore size distribution of solid catalysts.

Adsorption of gas by a porous material is described by an adsorption isotherm, the amount of adsorbed gas on the material at a constant temperature as a function of pressure. Porous materials are frequently characterized in terms of pore sizes derived

from sorption data. IUPAC conventions have been proposed for classifying pore sizes and gas sorption isotherms that reflect the relationship between porosity and sorption. The IUPAC classifications of adsorption isotherm are illustrated in Fig. 2.8.

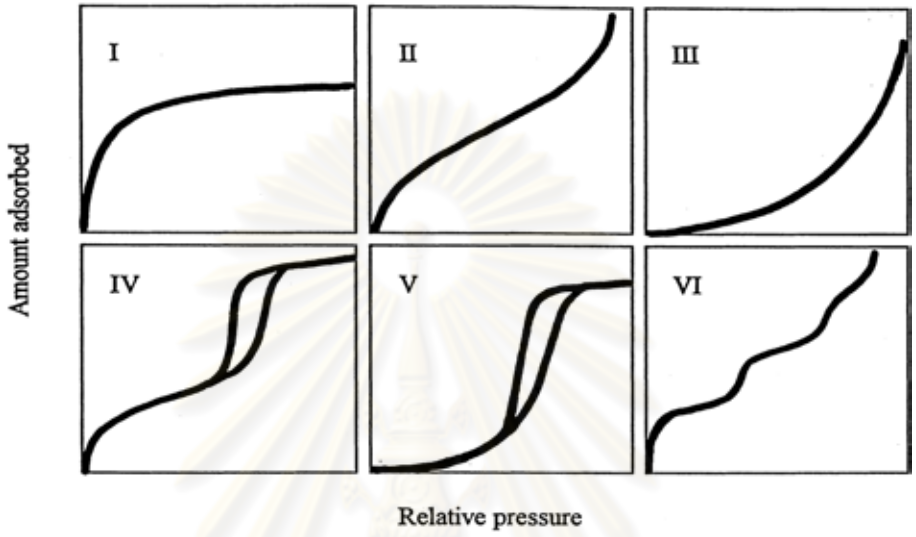

Figure 2.7 The IUPAC classification of adsorption isotherms [27].

Table 2.1 Features of adsorption isotherms

Type	**Features**	
	Interaction between sample surface and gas adsorbate	**Porosity**
I	Relatively strong	Micropore
II	Relatively strong	Nonporous
III	Weak	Nonporous
IV	Relatively strong	Mesopore
V	Weak	Mesopore
		Micropore
VI	Relatively strong Sample surface has an even distribution of energy	Nonporous

Table 2.1 shows the types and features of adsorption isotherms [28] and describes the adsorption isotherms based on the strength of the interaction between the sample surface and gas adsorbate and the existence or absence of pores.

Table 2.2 IUPAC classification of pores

Pore type	**Pore diameter (nm)**
Micropore	Up to 2
Mesopore	2 to 50
Macropore	50 or up

Pore types are classified as shown in Table 2.2. [28] Pore size distribution is measured by the use of nitrogen adsorption/desorption isotherm at liquid nitrogen temperature and relative pressures (P/P_0) ranging from 0.05-0.1. The large uptake of nitrogen at low P/P_0 indicates filling of the micropores (< 20 Å) in the adsorbent. The linear portion of the curve represents multilayer adsorption of nitrogen on the surface of the sample and the concave upward portion of the curve represents filling of mesopores and macropores.

The multipoint Brunauer, Emmett and Teller (BET) method is commonly used to measure total surface area.

$$\frac{1}{W[(P_0/P)-1]} = \frac{1}{W_mC} + \frac{C-1}{W_mC}(P_0/P)$$

Where W = weight of nitrogen adsorbed at a given P/P_0

W_m = weight of gas to give monolayer coverage

C = a constant that is related to the heat of adsorption.

A linear relationship between $1/W[(P/P_0)-1]$ and P/P_0 is required to obtain the quantity of nitrogen adsorbed. This linear portion of the curve is restricted to a limited portion of the isotherm, generally between 0.05-0.30. The slope and intercept are used to determine the quantity of nitrogen adsorbed in the monolayer and calculate the

surface area. For a single point method, the intercept is taken as zero or a small positive value, and the slope from the BET plot is used to calculate the surface area. The surface area reported depends upon the method used, as well as the partial pressure at which the data are collected.

2.9.3 Inductively coupled plasma-optical emission spectroscope (ICP-OES)

The inductively coupled plasma is a type of plasma source in which the energy is supplied by electromagnetic induction as shown in Fig. 2.9. The argon gas is typically used to create the plasma. The sample is nebulized within the nebulizer where it is atomized and introduced directly inside the plasma flame and break up into their respective atoms. The plasma torch consists of three concentric quartz tubes and a coil of the radio frequency (RF) generator (typically 1-5 kW at 27 MHz). When the torch is turned on, an intense magnetic field from the RF generator is turned on. The argon gas flowing through is ignited with a Tesla unit. The argon gas is ionized in those fields. A stable high temperature plasma at about 7000 K is then generated as the results of the inelastic collisions between the neutral argon atoms, created ions and free electrons [29].

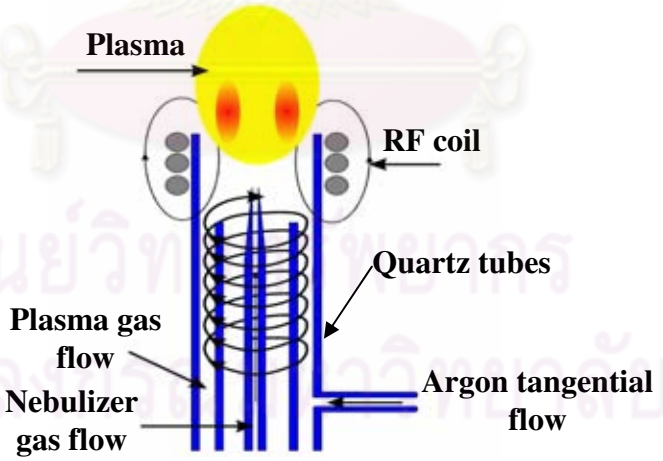

Figure 2.8 A typical plasma source [30].

ICP-OES is an emission spectrophotometric technique for elemental analysis exploiting. Electrons were excited and emit energy at a given wavelength as they return to ground state. The fundamental characteristic of this process is that each

element emits energy at wavelengths characteristic of a peculiar element. Although each element emits energy at multiple wavelengths, in the ICP-OES technique it is most common to select a single wavelength for a given element. The intensity of this emission is indicating of the amount of the element within the sample. Thus, by determining which wavelengths are emitted by a sample and by determining their intensities, the analyst can quantify the elemental composition of the given sample relative to a reference standard.

2.10 Friedel-Crafts acylation of aromatic compounds

Friedel-Crafts acylation is the attachment of acyl group to an aromatic ring in the presence of Lewis acid catalyst, such as $AlCl_3$, $FeCl_3$, $SnCl_4$. An intermediate losses a proton, then yields the acylated aromatic ring, in order to produce aromatic ketone. For example, the acylation of benzene with benzoyl chloride yields benzophenone.

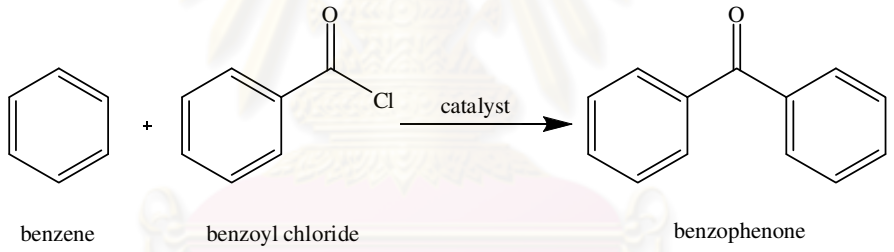

Scheme 2.4 Acylation of benzene with benzoyl chloride

ศูนย์วิทยทรัพยากร
จุฬาลงกรณ์มหาวิทยาลัย

CHAPTER III

EXPERIMENTAL

3.1 Starting materials

3.1.1 Clays

Clays (bentonite) were used as a raw material. Bentonite was kindly supported by Cernic International Co., Ltd. The compositions of bentonite are summarized in table 3.1.

Table 3.1 Bentonite compositions

Compositions	Bentonite[a]
SiO_2	63.60
Al_2O_3	17.60
MgO	-
Fe_2O_3	3.10
CaO	3.00
Na_2O	3.40
K_2O	0.50

[a] information from Cernic International Co., Ltd.

3.1.2 Chemicals

1. Sodium hydroxide, NaOH (Merck, reagent grade)
2. Sodium sulfate, Na_2SO_4 (Merck, analysis grade)
3. Hydrochloric acid, HCl (Merck, analysis grade)
4. Hydrofluoric acid, HF (Merck, analysis grade)
5. Sodium bicarbonate, $NaHCO_3$ (Merck, analysis grade)
6. Nitric acid, HNO_3 (Merck, analysis grade)
7. Aluminium chloride hexahydrate, $AlCl_3.6H_2O$ (Ajax Finechemical, AR grade)
8. Indium trichloride hydrate, $InCl_3.H_2O$ (Fluka Chemika, 39%)
8. Anisole (Laboratory reagent)
9. Benzene (Carlo Erba)

10. Toluene (Lab-Scan, reagent grade)
11. 1,3-dimethoxybenzene (Fluka Chemika, 98%)
12. Benzoyl chloride (Sigma-Aldrich, 99%)
13. Dioxane (Carlo Erba)
14. Ethyl acetate (Lab-Scan, reagent grade)
15. Dichloroethane (Laboratory reagent)
16. Dichloromethane (Lab-Scan, reagent grade)
17. Acetonitrile (Merck, analysis grade)
18. Hexane (Lab-Scan, reagent grade)
19. Acetone (commercial grade)

3.2 Instruments, apparatus and analytical measurements

3.2.1 Centrifuge

The purification of clays and the collection of the synthesized catalysts were processed by the centaur 2, Sanyo centrifuge. The purification of clays is aimed for removing quartz and other impurities.

3.2.2 Oven and furnace

Raw clays and all synthesized catalysts were dried in a Memmert UM-500 oven at 100°C for 24 h. The calcination was performed on a Carbolite RHF 1600 muffle furnace in air. Calcination of as-synthesized clays catalysts in air converted metal precursors in the interlayer of clays into metal oxide. The calcination condition for aluminium oxide-pillared clay was heating with the rate of 5°C /min and holding at 500°C for 1 h, whereas that of indium chloride impregnated aluminium oxide-pillared clay was heating with the rate of 5°C /min and holding at 450°C for 4 h.

3.2.3 X-ray diffractometer (XRD)

The XRD patterns and, in consequence, the basal spacing of catalysts (raw clays and modified clays catalysts) were identified using a Rigaku, Dmax 2200/utima plus X-ray powder diffractometer (XRD) with a monochromater and Cu K_{α} radiation (40 Kv, 30 mA). The 2-theta angle was ranged from 2 to 30 degree with the scan

speed of 3 degree/min and the scan step of 0.02 degree. The scattering slit, divergent slit and receiving slit were fixed at 0.5 degree, 0.5 degree and 0.15 mm, respectively.

3.2.4 X-ray fluorescence spectroscopy (XRF)

The amount of indium and chloride in the $InCl_3$ impregnated Al-pillared clays were analyzed using the Philips PW2400 X-ray fluorescence spectrometer at the Scientific and Technological Research Equipment Centre of Chulalongkorn University.

3.2.5 Inductively coupled plasma- optical emission spectroscopy (ICP-OES)

The amount of indium in the $InCl_3$ impregnated Al-pillared clays were analyzed using the Perkin Elmer PLASMA-1000 inductively couple plasma optical emission (ICP-OES) spectrometer at the Scientific and Technological Research Equipment Centre of Chulalongkorn University.

3.2.6 Nitrogen adsorptometer

The BET specific surface area of raw clays and synthesized catalysts were measured by using the Quantachrome Autosorb-l nitrogen adsorptometer. The 0.0400 g of clays was pretreatment at 300°C for 3 h. After that, the BET specific surface areas were obtained from nitrogen adsorption at 77 K.

3.2.7 Nuclear magnetic resonance spectroscopy (NMR)

The ^1H NMR spectra were obtained in $CDCl_3$ and determined by model Mercury plus 400 NMR spectrometer which operated at 399.84 MHz.

3.2.8 Chromatography

Thin layer chromatography (TLC) was carried on aluminium sheets precoated with silica gel (Merck's, kieselgel 60 PF254) in order to separate mixtures by eluting with ratio of hexane to ethyl acetate of 20:1.

Column chromatography was performed on silica gel (Merck's, kieselgel 60 G) in order to purify desired product by eluting with ratio of hexane to ethyl acetate of 40:1.

3.3 Homoionic clays

Homoionic clays were prepared by purification the raw clay and ion-exchange with the aqueous solution of sodium ions, following the method of Kanjanaboonmalert [31].

3.3.1 Purification of bentonite

Bentonite was purified by fractionated sedimentation. Thirty grams of bentonite were dispersed in 1,000 mL of deionized water under vigorous stirring for 3 h at room temperature. Then, quartz sediments were separated from the suspension of bentonite by centrifugation at 4,000 rpm for 10 min. The suspension of bentonite was dried at 100°C for 48 h to obtain pure montmorillonite. Montmorillonite character was confirmed by XRD measurement.

3.3.2 Na-ion exchange

Na-montmorillonite was prepared by cation exchange. Montmorillonite from the previous step was suspended in 5 M NaOH with ratio of clay to NaOH solution of 1 g: 50 mL for 24 h at room temperature. The above process was repeated three times. The hydroxide ions and the excess sodium ions were removed from Na-montmorillonite using a dialysis membrane (Seamless Cellulose Tubing, small size 30, Wako Chemicals USA). Then the products were dried at 100°C. The Na-montmorillonite was characterized by XRD technique.

3.4 Synthesis of aluminium oxide-pillared clay (Al-PLC) [32]

2 g of Na-montmorillonite was dispersed into 100 mL water under stirring for 48 h at room temperature. The Al-pillar agent was prepared by adding 0.2 M NaOH to 0.2 M $AlCl_3$ with the ratio of OH/Al was 1.9 and stirring for 24 h at room temperature. The Al-pillar agent was then slowly added to the prepared clay suspension with the ratio of Al/clay of 3.8 mol/Kg. The mixture was stirred for 24 h at room temperature. After that, the precipitates were collected by centrifugation at 4,000 rpm for 10 min and washed with distilled water until free of chloride ion. The intercalate product (Al-PLC) was dried at 100°C for 24 h and calcined at 500°C at the rate 5°C /min for 1 h.

3.5 Synthesis of indium chloride impregnated aluminium oxide-pillared clay ($InCl_3$/Al-PLC)

Indium chloride impregnated aluminium oxide-pillared clay was synthesized by following the previous work of Masaleh [33]. The aluminium oxide-pillared clay was impregnated using a solution of 2% $InCl_3$ in ethanol. The slurry mixture was dried at 60°C and calcined with the rate of 5°C /min and holding at 450°C for 4 h. The product was named $InCl_3$/Al-PLC.

3.6 Sample preparation for ICP

The 0.0400g of a calcined catalyst, placed in a 100 mL teflon beaker, was soaked with 10 mL concentrated HCl and subsequently with 10 mL of 48% HF in order to remove silica in the form of volatile SiF_4 species. The mixture was heated but not boiled to dryness on a hot plate. The removal of silica was repeated three times. Then, 10 mL of 6 M HCl: 6 M HNO_3 mixtures in the ratio of 1:3 was added and further heated to dryness. 5 mL of 6 M HCl was added and the mixture was warmed for 5 min to complete dissolution. The solution was transferred to 50 mL polypropylene volumetric flask and made up its volume by adding deionized water. If the sample was not analyzed immediately, the solution was then transferred into a plastic bottle with a treated cap underlined with a polypropylene seal.

3.7 Optimum conditions study on Friedel-Crafts acylation of anisole with benzoyl chloride

3.7.1 General procedure

A typical reaction mixture was consisted of 0.01 mmol catalyst, anisole, benzoyl chloride and 0.5 mL dioxane in a round bottom flask connected with a condenser for refluxing under N_2 gas. The mixture was continuously stirred. After that, the catalyst was filtered out of the reaction mixture. The product was analyzed by NMR.

3.7.2 Effect of mole ratio of anisole to benzoyl chloride

The Friedel-Crafts acylation was carried out according to the general procedure, but the mole ratio of anisole to benzoyl chloride was changed to 1:1, 1:2, 1:3, 1:4 and 1:5 mmol.

3.7.3 Effect of the amount of catalyst

The Friedel-Crafts acylation was carried out according to the general procedure, but the amount of $InCl_3$ impregnated on Al-PLC was changed to 0.01, 0.02, 0.03, 0.04 and 0.05 mmol.

3.7.4 Effect of reaction time

The Friedel-Crafts acylation was carried out according to the general procedure, but the reaction time of Friedel-Crafts acylation was changed to 1, 2, 3, 4 and 5 h.

3.7.5 Effect of type of organic solvents

The Friedel-Crafts acylation was carried out according to the general procedure, but using different organic solvents, such as dioxane, dichloromethane, dichloroethane, ethyl acetate and acetonitrile.

3.8 The screening of substrates

3.8.1 Variation of aromatic compounds

The general procedure using $InCl_3$/Al-PLC as a catalyst and dioxane as a solvent at reflux temperature for 4 h was carried out. Anisole, benzene, toluene and 1,3-dimethoxybenzene were tested as different aromatic compounds.

3.8.2 Variation of acid chlorides

The general procedure using $InCl_3$/Al-PLC as a catalyst and dioxane as a solvent at reflux temperature for 4 h was carried out. The type of acid chloride was varied as the followings: benzoyl chloride, acetyl chloride, butyryl chloride and 4-ethylbenzoyl chloride.

3.9 Reuse of catalyst

The used $InCl_3$/Al-PLC was regenerated by calcination at 450°C for 4 h. The structural characterization of the regenerated $InCl_3$/Al-PLC catalyst was characterized using XRD, N_2-adsorption/desorption and ICP-OES techniques. Then, the regenerated $InCl_3$/Al-PLC was used as a catalyst in the Friedel-Crafts acylation again.

ศูนย์วิทยทรัพยากร
จุฬาลงกรณ์มหาวิทยาลัย

CHAPTER IV

RESULTS AND DISCUSSION

4.1 The characterization of clays

Clays was characterized by X-ray diffraction (XRD). This technique was used to investigate the changes of clay structure, emphasizing on a basal spacing and the intensity of d_{001} reflection.

4.1.1 The characterization of raw bentonite

Bentonite is phyllosilicate-typed clay, generally containing montmorillonite and impurities such as calcite, quartz, feldspars, crystobalite and humic acids. Quartz is the major impurity of clay minerals that causes clay having low surface area and acidic site, which reduce the catalytic efficiency of clay. The characteristic structure of raw bentonite analyzed by XRD technique is shown in Fig. 4.1. The pattern shows the characteristic peaks of montmorillonite at 2θ of 7° and 19°, corresponding to the 001 and 100 planes of montmorillonite respectively [34]. The d_{001} basal spacing is 13.46 Å. The peaks at 2θ of 22°, 24° and 27° were assigned to quartz (SiO_2) [34].

ศูนย์วิทยทรัพยากร
จุฬาลงกรณ์มหาวิทยาลัย

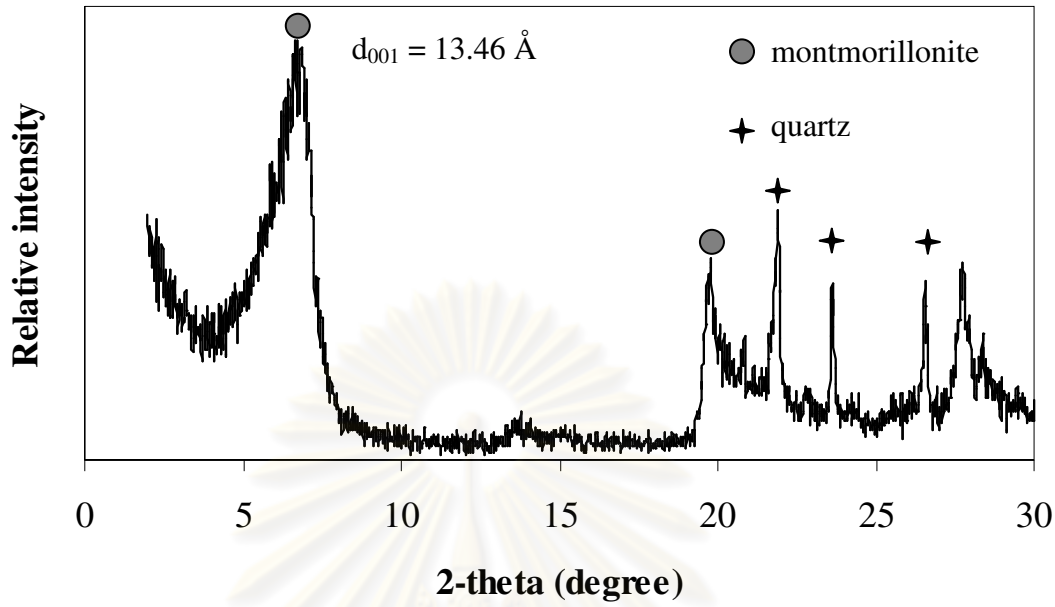

Figure 4.1 XRD pattern of raw bentonite.

4.2 The synthesis and characterization of homoionic clay

Homoionic clay was prepared by ion exchange after purification. In the purification process, quartz and other impurities were removed from bentonite by dispersion and centrifugation process. The Na ions were intercalated between the clay layers in order to obtain homoionic clay, used as the starting material for synthesis of the clay catalysts.

4.2.1 The purification of bentonite

Bentonite was dispersed in water that makes its volume largely expand. Raw bentonite contains montmorillonite as main constituent and other impurities. These impurities could be removed by repetitive dispersion and centrifugation processes. Only montmorillonite was left in a residue and the sample was designated as montmorillonite.

The X-ray diffraction patterns of raw bentonite and montmorillonite are shown in Fig 4.2. The quartz peak at 2θ of 22°, 24° and 27° disappeared in the XRD pattern of montmorillonite collected from the dispersion and centrifugation of clay suspension in water, suggesting quartz and other impurities were removed from raw

bentonite. The structure of montmorillonite clay was still remained and the (001) peak was found at the 2θ of 7°, corresponding to the d_{001} spacing of 12.34 Å.

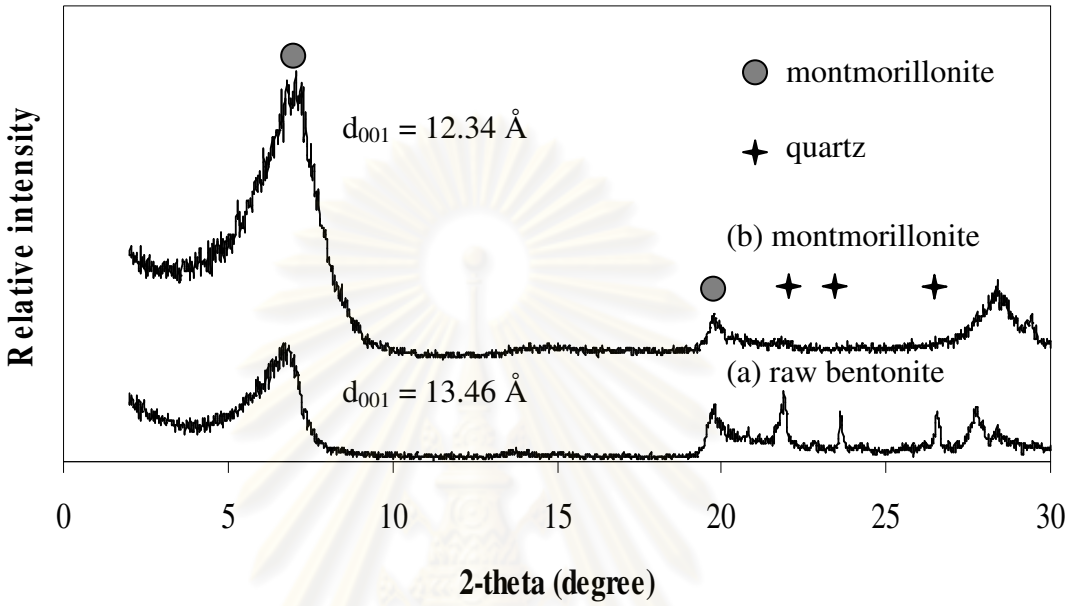

Figure 4.2 XRD patterns of (a) raw bentonite and (b) montmorillonite.

4.2.2 Na-ion exchange of montmorillonite

Layer structure of clay possesses a net negative charge, which balanced with interlayer cations, such as Na or K ions. The presence of sodium as the predominant exchangeable cation can result in the clay swelling to several times of its original volume, due to the large solvation energy of sodium ion (98 kcal/mol) [35] and its small electrostatic interaction between monovalent cations and negatively layer charge. Montmorillonite treated with 5 M NaOH for three times, was chosen as starting homoionic clay and designated as Na-montmorillonite.

The X-ray diffraction patterns of Na-montmorillonite and purified bentonite (as montmorillonite) are shown in Fig. 4.3. The d_{001} spacing of Na-montmorillonite was 15.38 Å. The peak of Na-montmorillonite was shifted to the left as compared to that of purified bentonite, indicating that Na^+ ions that were surrounded with water molecules intercalated into the clay layer. As previously mentioned that sodium ion

has large solvation energy, more water molecules were solvated sodium interlayer cations, causing the larger d-spacing of Na-montmorillonite.

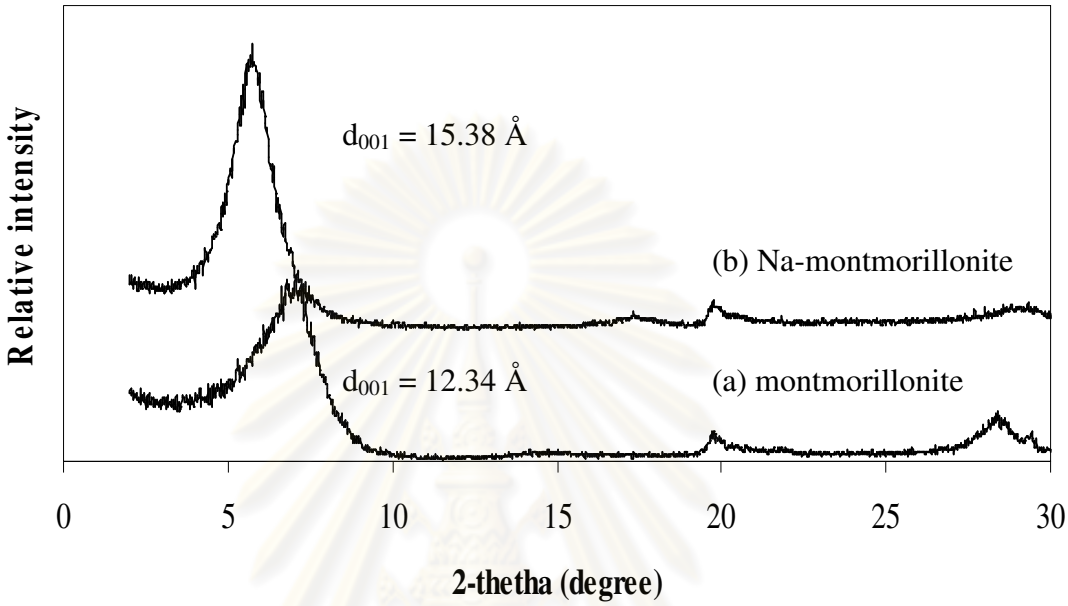

Figure 4.3 XRD patterns of (a) montmorillonite and (b) Na-montmorillonite.

4.3 The characterization of aluminium oxide-pillared clay (Al-PLC)

The XRD patterns of Al-PLC and Na-montmorillonite are shown in Fig. 4.4. The d_{001} spacing of Al-PLC was found as a broad peak with the high intensity at 17.51Å. The 2θ peak of Al-PLC shifted slightly to the larger basal spacing and was broader comparing with the d_{001} peak of Na-montmorillonite, explaining that the sodium ion within the layer of montmorillonite can be exchanged by aluminium polyoxocations. The aluminium polyoxocation $[Al_{13}O_4(OH)_{24}(H_2O)_{12}]^{7+}$ (Keggin structure as shown in appendices Fig. A-1) [36], prepared by adding 0.2 M NaOH to 0.2 M $AlCl_3$ with the ratio of OH/Al was 1.9, intercalated into the clay layer and converted to the aluminium oxide pillars during calcination process. The transformation of aluminium polyoxocations into rigid aluminium oxide pillars, tightly bound to the clay layer, increased the disordering within interlayer spacing of clay structure.

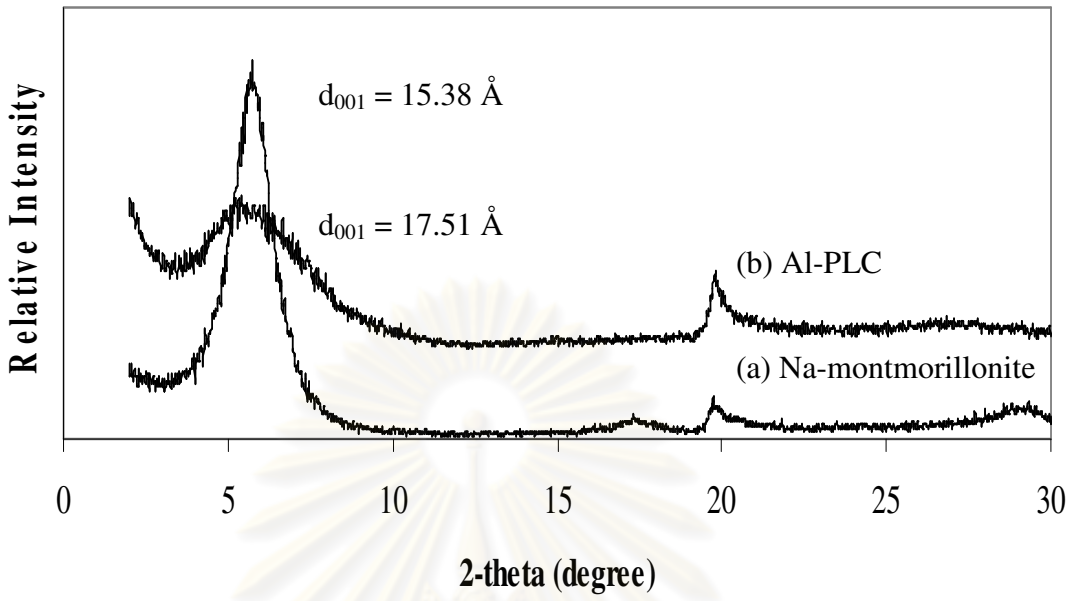

Figure 4.4 XRD patterns of (a) Na-montmorillonite and (b) aluminium oxide-pillared clay (Al-PLC).

4.4 The characterization of indium chloride impregnated aluminium oxide-pillared clay ($InCl_3$/Al-PLC)

The XRD patterns of $InCl_3$/Al-PLC and Al-PLC are shown in Fig. 4.5. The d_{001} spacing of $InCl_3$/Al-PLC was around 16.54 Å which is a little bit lower than that of Al-PLC, but a lot broader, indicating that the recalcination process caused the structure collapse slightly and the impregnation of $InCl_3$ increased the disordering between the interlayer spacing of clay. Furthermore, the characteristic peak of bulk $InCl_3$ assigned in Fig. 4.6 (database JCPDS: 34-1145) does not appear in the XRD pattern of $InCl_3$/Al-PLC. This result indicates that small crystals of $InCl_3$ distribute insides pillared clay structure. The amount of $InCl_3$ was reported in section 4.5 at ~2%.

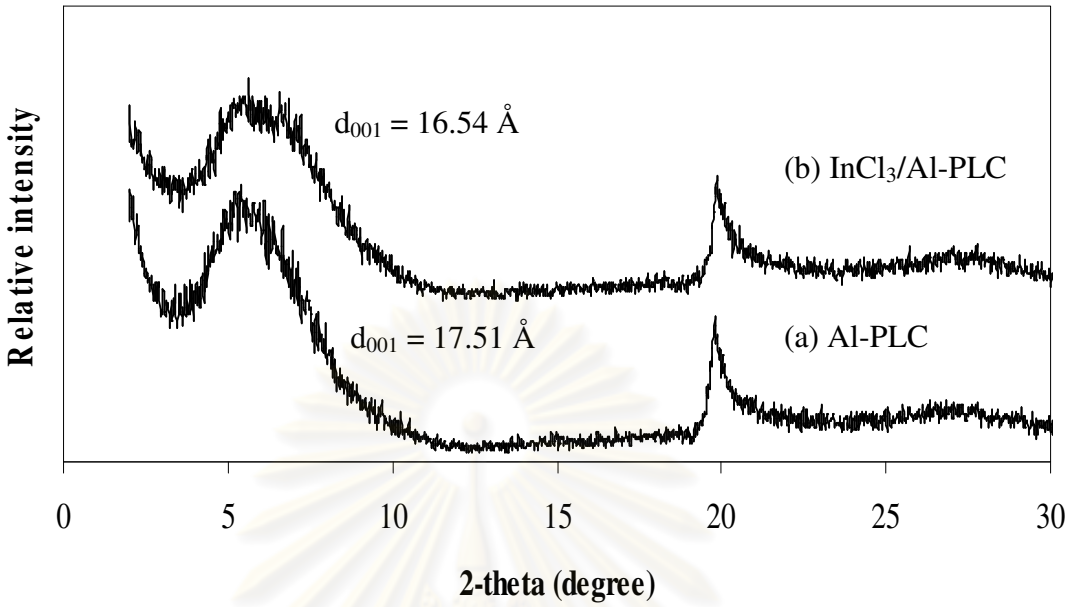

Figure 4.5 XRD patterns of (a) aluminium oxide-pillared clay (Al-PLC) and (b) indium chloride impregnated aluminium oxide-pillared clay ($InCl_3$/Al-PLC).

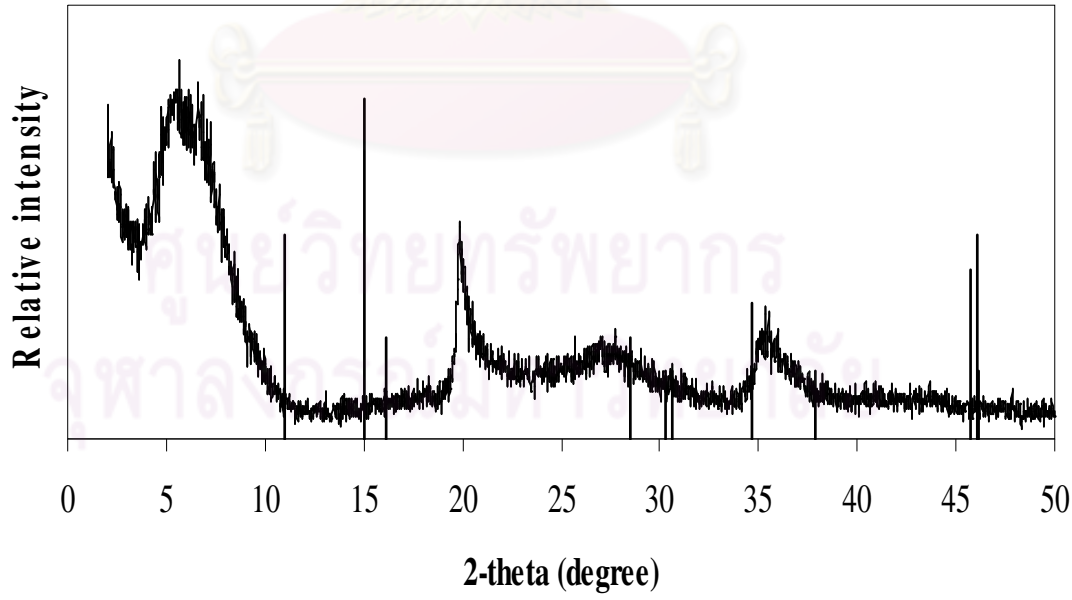

Figure 4.6 Simulation of XRD patterns of indium trichloride ($InCl_3$) from database JCPDS: 34-1145.

4.5 Determination of indium and chloride contents

Table 4.1 shows the indium chloride contents in $InCl_3$/Al-PLC catalyst. Indium and chloride contents were analyzed by XRF and the mole of indium to chloride was found at 1:3. The indium content was also analyzed by ICP. Indium chloride was not found in the composition of starting montmorillonite as expected. The indium chloride content in Al-PLC was 1.99 wt%, and this value used in further calculation during the catalytic experiments.

Table 4.1 The indium and chloride contents in clays sample

Samples	Wt% of $InCl_3$ content[a]	Wt% of $InCl_3$ content[b]
Montmorillonite	-	not detected
$InCl_3$/Al-PLC	2.23	1.99
	(In 1.16 wt%, Cl 1.07 wt%)[c]	(In 1.03 wt%)[c]

[a] The chloride content was analyzed by XRF.

[b] The indium content was analyzed by ICP.

[c] The numbers in parentheses are raw data.

4.6 Nitrogen adsorption/desorption (BET)

The BET specific surface area of raw bentonite, montmorillonite and Al-PLC are compared in Table 4.2. Al-PLC showed higher specific surface area (209.41 m^2/g) that is higher the surface area of montmorillonite. The increase of surface area relates to the increase of the d_{001} spacing from 12.34 to 16.96 Å. The interlayer of aluminium oxide popped up the clay gallery height and allowed more access of nitrogen probe molecules. Furthermore, clay-layered structure (2-dimensional structure) was converted to mesoporous structure (3-dimensional structure) by connecting the adjacent aluminosilicate layers with the aluminium oxide pillars in the interlayered region. This result also confirmed the XRD results that Al_2O_3 in the prepared aluminium oxide-pillared clay was distributed inside the interlayer of montmorillonite instead of aggregation outside the clay structure. If the Al_2O_3 presents as a bulk Al_2O_3 outside the clay structure, the surface area would be similar to or lower than that of montmorillonite.

Table 4.2 BET specific surface area

Samples	BET specific surface area (m^2/g)
Raw bentonite	59.86
Montmorillonite	69.83
Al-PLC	209.41
$InCl_3$/Al-PLC	187.23

$InCl_3$/Al-PLC showed higher specific surface area than montmorillonite but lower than Al-PLC. This could be explained that $InCl_3$ deposited on the pore wall of the aluminium oxide-pillared clay and occupied the void in mesoporous structures, causing the specific surface area reduced. The nitrogen adsorption/desorption isotherms of all sample, as shown in appendices (Fig. A-2 to A-5), revealed the type IV isotherm, which indicating the micro-mesoporous structure.

4.7 Catalytic activity of Al-PLC and $InCl_3$/Al-PLC for Friedel-Crafts acylation

Friedel-Crafts acylation of anisole with benzoyl chloride was selected for testing the catalytic activity of synthesized Al-PLC and $InCl_3$/Al-PLC.

4.7.1 Activity of montmorillonite, Al-PLC and $InCl_3$/Al-PLC catalysts in Friedel-Crafts acylation of anisole with benzoyl chloride

In this project, the Friedel-Crafts acylation used the 1:3 mole ratio of anisole to benzoyl chloride and 0.0597 g catalysts in 1,4-dioxane. The reaction was carried out under refluxing for 4 h. The results are presented in Table 4.3.

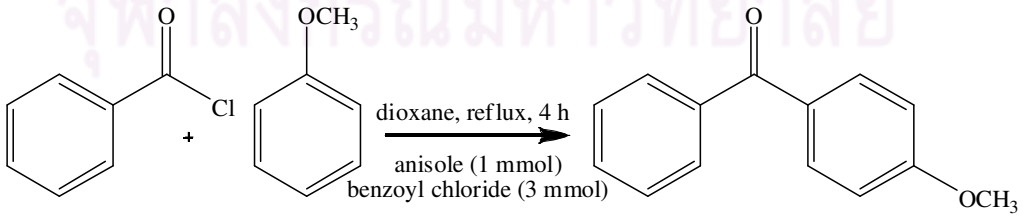

4-MBP

Table 4.3 Activities of various catalysts in Friedel-Crafts acylation

Entry	Catalysts	% Yield[a]
1	None	0
2	Montmorillonite	< 10
3	Al-PLC	18
4	$InCl_3$/Al-PLC	56

[a] The yield was quantified by ^{1}H-NMR using toluene as an internal standard.

From Table 4.3, the catalytic activity of $InCl_3$/Al-PLC is compared to those of montmorillonite, Al-PLC and without a catalyst. Both Al-PLC and $InCl_3$/Al-PLC showed higher activities than the montmorillonite, relating to their significantly higher surface area. The Al-PLC popped up the gallery high of clay structure, allowing the access of substrates into the interlayer region. Moreover, acylation could be catalyzed by Lewis acid, and Al-PLC possesses higher Lewis acidity than the montmorillonite [37]. Despite the lower surface area than Al-PLC, $InCl_3$/Al-PLC showed higher activity. The high acylation activity was attributed to the redox reaction of $InCl_3$/Al-PLC. The redox property of catalyst ($E^0_{In^{3+}/In^{1+}}$ = -0.44V) [13] results to the high yield of 4-MBP.

The proposed mechanism describing the catalysis of Friedel-Crafts acylation is shown in Scheme 4.1. The redox mechanism of Friedel-Crafts acylation was similar to the previous report of $InCl_3$/Si-MCM-41 [13].

ศูนย์วิทยทรัพยากร
จุฬาลงกรณ์มหาวิทยาลัย

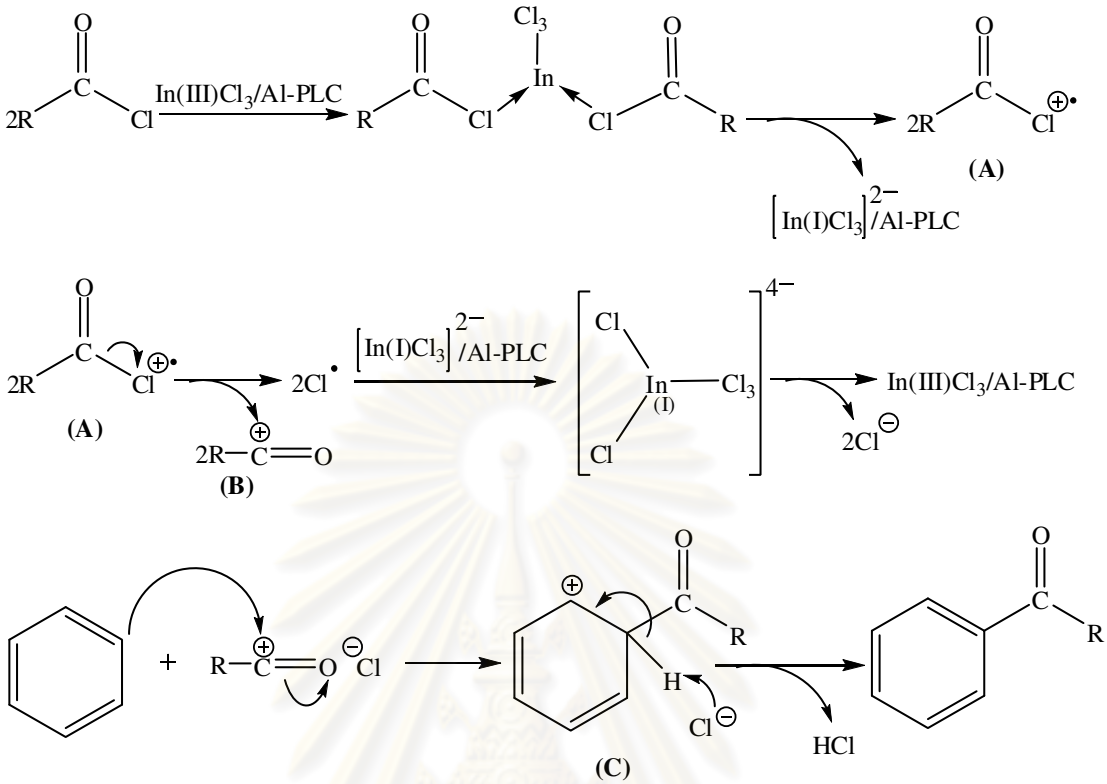

Scheme 4.1 Mechanism of Friedel-Crafts acylation of aromatic compounds on $InCl_3$/Al-PLC.

The first step, acid chlorides are oxidized by In(III)Cl_3/Al-PLC to form intermediates **(A)**, charge transfer of **(A)** should be formed which loses chloride radicals and give carbocations **(B)** act as electrophiles. The chloride radicals are reduced by $[In(I)Cl_3]^{2-}$/Al-PLC to form chloride ions and the active In(III)Cl_3/Al-PLC catalyst is regenerated. The aromatic C=C as a nucleophile, attacks the electrophilic carbocation. This step destroyed the aromaticity giving the cyclohexadienyl cation intermediate **(C)**. Removal of the proton form the carbon bearing the acyl group reformed the C=C and the aromatic system, generated HCl.

4.7.2 Study on the optimum condition for Friedel-Crafts acylation of anisole with benzoyl chloride by $InCl_3$/Al-PLC

As shown in the previous section, $InCl_3$/Al-PLC showed good activity towards the model reaction; therefore, it is further investigated to find the optimized condition in Friedel-Crafts acylation. The mole ratio of anisole to benzoyl chloride, the amount of the catalyst, reaction time and the types of organic solvents were varied to search for the optimized condition.

4.7.2.1 Effect of the mole ratio of anisole to benzoyl chloride

The reaction of anisole with various amounts of benzoyl chloride with the fixed amount (1 mmol) of anisole was experimented. The results are presented in Table 4.4.

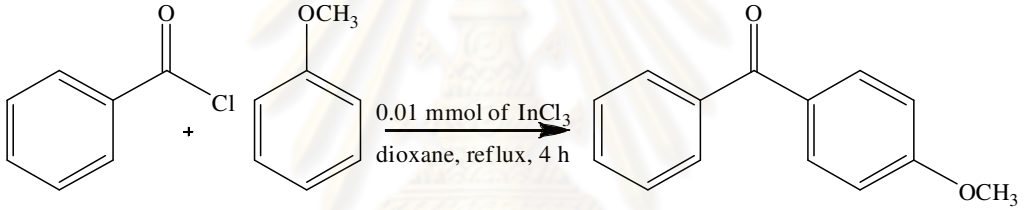

4-MBP

Table 4.4 Effect of mole ratio of anisole to benzoyl chloride

Entry	Anisole:Benzoyl chloride (mmol)	% Yield[a]
1	1:1	24
2	1:2	30
3	1:3	56
4	1:4	43
5	1:5	45

[a] The yield was quantified by ^{1}H-NMR using toluene as an internal standard.

From Table 4.4, the yields of 4-MBP were increased with increasing the amount of benzoyl chloride (entries 1-3). But, the yields were decreased from 56 to 45% when the amount of benzoyl chloride was raised to the mole ratio of 1:4 and 1:5 (entries 4-5). The higher amount of benzoyl chlorides increased the number of carbocations that might attack anisole at several positions and generated the by-products. Therefore, the mole ratio of 1:3 was chosen for further experiments.

4.7.2.2 Effect of the amount of catalyst

The amount of catalyst normally influences the performance of the reaction. In this part, the amount of $InCl_3$/Al-PLC catalyst was varied according to the actual amount of $InCl_3$ in the catalyst. The results are summarized in Table 4.5.

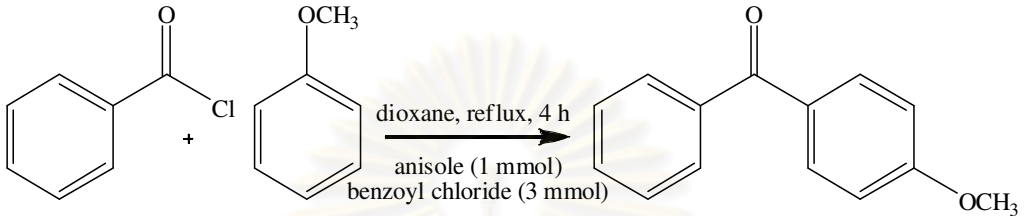

4-MBP

Table 4.5 Effect of the amount of $InCl_3$ in $InCl_3$/Al-PLC

Entry	Weight of catalyst (g)	$InCl_3$ in $InCl_3$/Al-PLC (mmol)	% Yield[a]
1	0.0597	0.01	56
2	0.1194	0.02	75
3	0.1790	0.03	91
4	0.2387	0.04	92
5	0.2984	0.05	94

[a] The yield was quantified by ^{1}H-NMR using toluene as an internal standard.

As shown in Table 4.5, the yields of 4-MBP increased with increasing the amount of the catalysts. The highest yield of 4-MBP was obtained when $InCl_3$ increased to 0.05 mmol. However, there were small increases in the yield of 4-MBP at 0.03 to 0.05 mmol (entries 3-5); therefore, the amount of $InCl_3$/Al-PLC with $InCl_3$ of 0.03 was fixed for further investigation.

4.7.2.3 Effect of the reaction time

The Friedel-Crafts acylation was carried out from 1 h to 5 h and the results of various reaction times are summarized in Fig. 4.7.

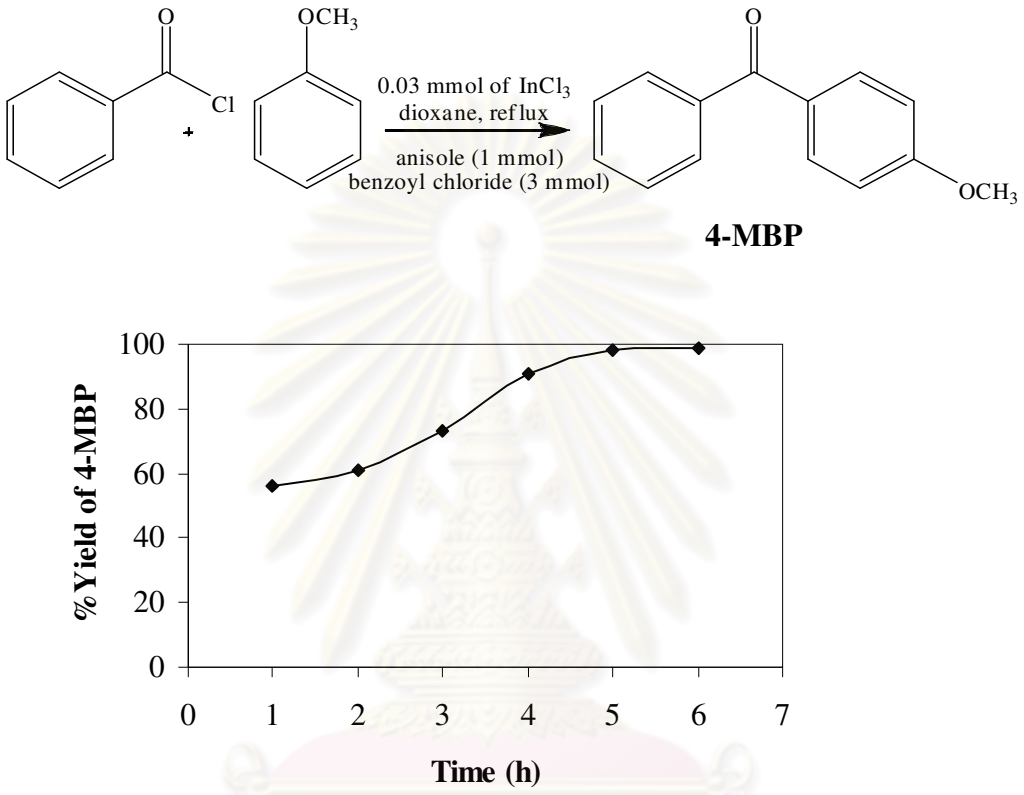

Figure 4.7 Effect of reaction time on the percent yield of 4-MBP.

When the reaction time decreased, %yield of 4-MBP decreased significantly from 99 to 56%. From Fig. 4.7, the product yields increased exponentially with the reaction time until 4 h. After 4 h, the yield was constant. Therefore, the reaction time at 4 h was chosen for further experiments.

4.7.2.4 Effect of the type of organic solvents

The effect of organic solvents on Friedel-Crafts acylation was carried out using the 1:3 mmol of anisole to benzoyl chloride and $InCl_3$/Al-PLC catalyst with the equivalent of 0.03 mmol $InCl_3$ under the reflux condition for 4 h. The results are described in Table 4.6.

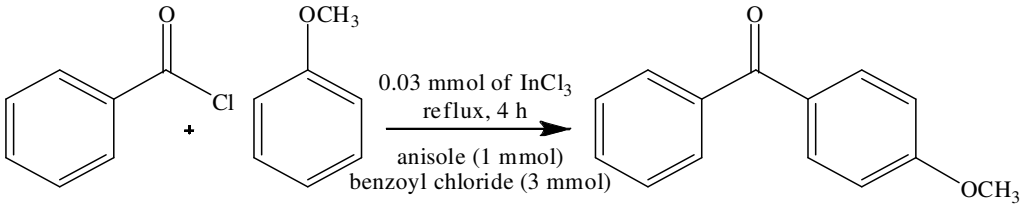

4-MBP

Table 4.6 Effect of the type of organic solvents

Entry	Organic solvent	Dipole moment [38]	% Yield[a]
1	1,4-dioxane	0.45	91
2	1,2-dichloroethane	1.50	65
3	Dichloromethane	1.60	54
4	Ethyl acetate	1.78	47
5	Acetonitrile	3.92	20

[a] The yield was quantified by ^{1}H-NMR using toluene as an internal standard.

As shown in Table 4.6, the yield of 4-MBP was high with 1,4-dioxane (entry 1) as a solvent. Other solvents, such as dichloromethane, 1,2-dichloroethane and ethyl acetate (entries 2-4), gave 4-MBP in moderate yields, while acetonitrile gave 4-MBP in low yield (entries 5). This result could be the effect of the dipole moment of the solvent. The 1,4-dioxane solvent possesses the lowest polarity among these solvents. The more polar solvent, the stronger its coordination with the carbocation intermediate. The stronger coordination would block the access of nucleophilic aromatics to attack the carbocation [39]. Therefore, in this work, 1,4-dioxane was the most suitable solvent.

4.7.3 The screening of substrates

From the last section, the reaction of anisole (1 mmol), benzoyl chloride (3 mmol) and the amount of $InCl_3$/Al-PLC catalyst with the equivalent of 0.03 mmol $InCl_3$ in 1,4-dioxane at reflux temperature for 4 h was applied as the optimized condition in Friedel-Crafts acylation for the screening of both aromatic compounds and acid chlorides.

4.7.3.1 Type of aromatic compounds

The variation of aromatic compounds under the optimized condition was carried out and the results are described in Table 4.7.

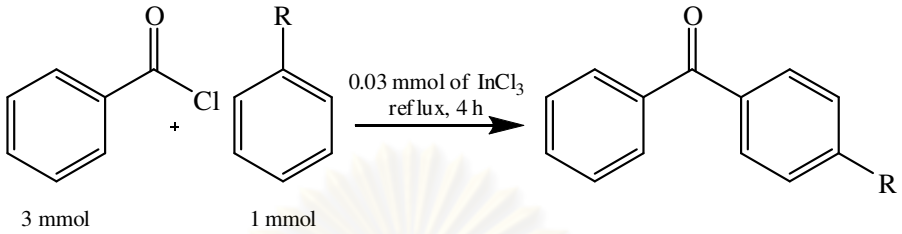

Table 4.7 Synthesis of aromatic ketones from various aromatic compounds under the optimal condition

Entry	Aromatic compound	% Yield[a]
1	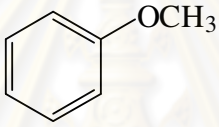	91
2	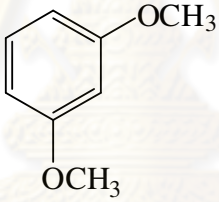	84
3	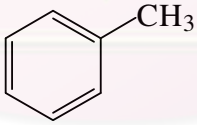	56[b]
4	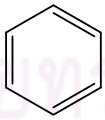	27

[a] The yield was quantified by ^{1}H-NMR using toluene as an internal standard.

[b] The yield was quantified by ^{1}H-NMR using acetonitrile as an internal standard.

The Friedel-Crafts acylation of benzoyl chloride with aromatic compounds such as anisole and 1,3-dimethoxybenzene gave high yields of aromatic ketone (entries 1-2), while the reaction with toluene gave moderate yield (entry 3). The reaction of 1,3-dimethoxybenzene gave slightly lower activity than that of anisole, possibly caused by its steric effect. For the moderate activity in the case of toluene, it probably results from methyl group which is considered as the weakly electron

donating group. In the case of benzene, the acylation was difficult to accomplish and led to the lower yield of aromatic ketone (entry 4) because the lack of an electron donating group. The electron donating group added electron density to the aromatic ring, making it more nucleophilic aromatics which strongly attack to the carbocation intermediate.

4.7.3.2 Type of acid chlorides

The variation of acid chlorides under the optimized condition was carried out and the results are described in Table 4.8.

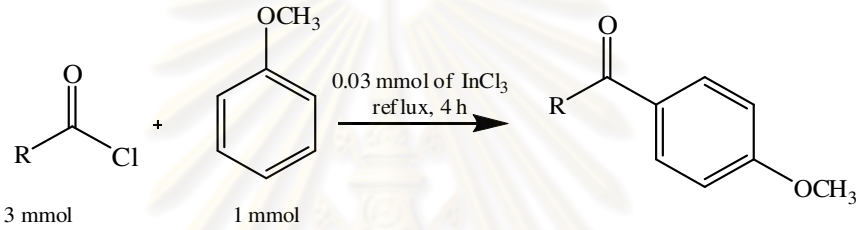

Table 4.8 Synthesis of aromatic ketones from various acid chlorides under the optimal condition

Entry	Acid chloride	% Yield[a]
1	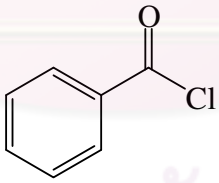	91
2	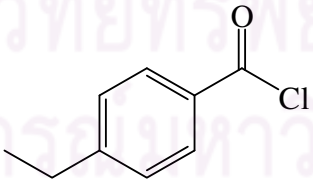	83
3	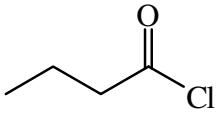	87
4	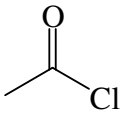	89[b]

[a] The yield was quantified by ^{1}H-NMR using toluene as an internal standard.

[b] The yield was quantified by ^{1}H-NMR using acetonitrile as an internal standard.

In Table 4.8, various acid chlorides as substrates could be converted to aromatic ketones in high yields. Both aromatic (entries 1-2) and aliphatic (3-4) acid chlorides were furnished to the corresponding aromatic ketones in excellent yields. Due to the acylation occurred at the carbonyl position; using either aromatic or aliphatic acids results to similar percent yields.

All products were presented in table 4.9 and their identities were characterized by ^{1}H NMR. The ^{1}H-NMR spectra are shown in the appendices (Fig. A-7 to A-13).

Table 4.9 Products obtained from various aromatic compounds and acid chlorides

	RCOR′ (variation of aromatic compounds)		**R′COR (variation of acid chlorides)**
1	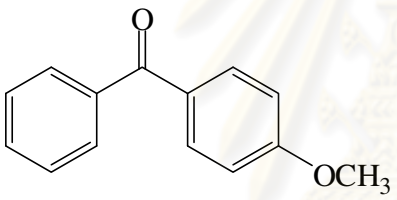	**5**	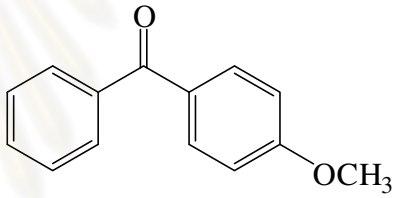
2	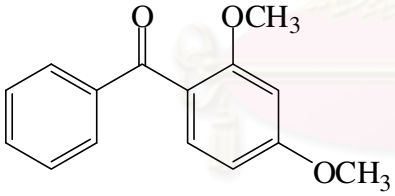	**6**	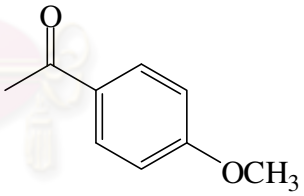
3	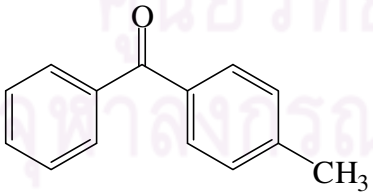	**7**	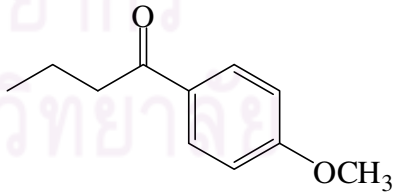
4	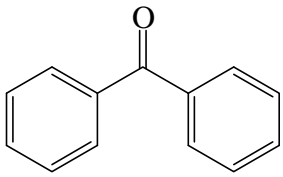	**8**	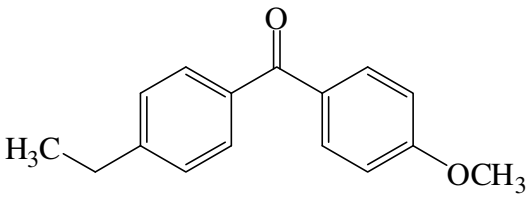

4-methoxybenzophenone (1 = 5); ^{1}H NMR ($CDCl_3$) δ (ppm): 3.84 (3H, s, ArOC**H$_3$**), 6.93 (2H, d, *J* = 8.67 Hz, Ar**H**), 7.45 (2H, t, *J* = 7.37 Hz, Ar**H**), 7.53 (1H, t, *J* = 7.26 Hz, Ar**H**), 7.69 (2H, d, *J* = 7.43 Hz, Ar**H**), 7.78 (2H, d, *J* = 8.72 Hz, Ar**H**).

2,4-dimethoxybenzophenone (2); ^{1}H NMR ($CDCl_3$) δ (ppm): 3.65 (3H, s, ArOC**H$_3$**), 3.82 (3H, s, ArOC**H$_3$**), 7.12 (1H, d, *J* = 7.83 Hz, Ar**H**), 7.45 (1H, d, *J* = 7.65 Hz, Ar**H**), 7.53 (3H, t, *J* = 7.26 Hz, Ar**H**), 7.60 (1H, s, Ar**H**), 7.78 (2H, d, *J* = 7.05 Hz, Ar**H**).

4-methylbenzophenone (3); ^{1}H NMR ($CDCl_3$) δ (ppm): 2.42 (3H, s, ArC**H$_3$**), 7.25 (2H, t, *J* = 7.84 Hz, Ar**H**), 7.44 (1H, t, *J* = 7.26 Hz, Ar**H**), 7.56 (2H, t, *J* = 7.43 Hz, Ar**H**), 7.70 (2H, d, *J* = 8.12 Hz, Ar**H**), 7.74 (2H, d, *J* = 6.95 Hz, Ar**H**).

Benzophenone (4); ^{1}H NMR ($CDCl_3$) δ (ppm): 7.44 (2H, t, *J* = 7.12 Hz, Ar**H**), 7.56 (4H, t, *J* = 7.10 Hz, Ar**H**), 7.78 (4H, d, *J* = 8.12 Hz, Ar**H**).

4-methoxyacetophenone (6); ^{1}H NMR ($CDCl_3$) δ (ppm): 2.62(3H, s, C**H$_3$**C=O), 3.85 (3H, s, ArOC**H$_3$**), 6.94 (2H, d, *J* = 8.62 Hz, Ar**H**), 7.85 (2H, d, *J* = 8.74 Hz, Ar**H**).

4-methoxybutyrophenone (7); ^{1}H NMR ($CDCl_3$) δ (ppm): 0.96 (3H, t, *J* = 7.41 Hz, CH_2C**H$_3$**), 1.64 (2H, q, *J* = 7.32 Hz, CH_2C**H$_2$**CH_3), 2.97 (2H, t, *J* = 7.37 Hz, CH_2C**H$_2$**C=O), 3.85 (3H, s, ArOC**H$_3$**), 6.93 (2H, d, *J* = 8.65 Hz, Ar**H**), 7.86 (2H, d, *J* = 8.70 Hz, Ar**H**).

4-ethyl,(4-methoxybenzophenone) (8); ^{1}H NMR ($CDCl_3$) δ (ppm):): 1.24 (3H, t, *J* = 7.21 Hz, CH_2C**H$_3$**), 2.62 (2H, q, *J* = 7.24 Hz, CH_3C**H$_2$**), 3.85 (3H, s, ArOC**H$_3$**), 6.94 (2H, d, *J* = 8.51 Hz, Ar**H**), 7.25 (2H, d, *J* = 8.23 Hz, Ar**H**), 7.66 (2H, d, *J* = 7.39 Hz, Ar**H**), 7.82 (2H, d, *J* = 8.21 Hz, Ar**H**).

ศูนย์วิทยทรัพยากร
จุฬาลงกรณ์มหาวิทยาลัย

4.8 Regenerated catalysts

4.8.1 The characterization of the regenerated catalyst

The regenerated $InCl_3$/Al-PLC and $InCl_3$/Al-PLC catalysts were characterized by XRD, and their patterns are shown in Fig. 4.8.

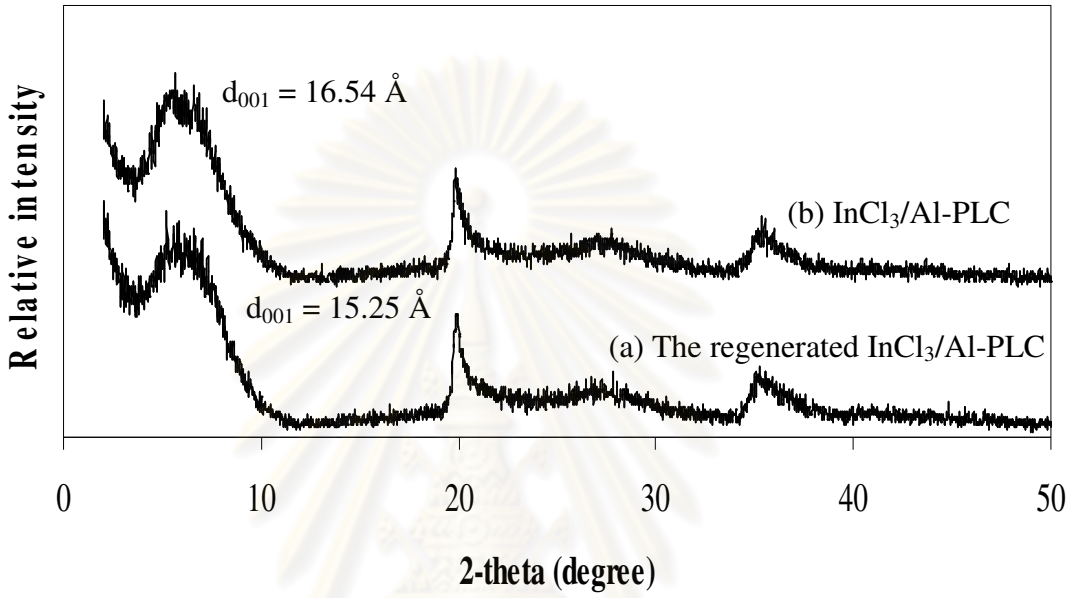

Figure 4.8 XRD patterns of (a) regenerated $InCl_3$/Al-PLC and (b) $InCl_3$/Al-PLC.

Table 4.10 Indium chloride content and BET specific surface area of regenerated $InCl_3$/Al-PLC and $InCl_3$/Al-PLC

Samples	Wt% of $InCl_3$ content	BET specific surface area (m^2/g)
$InCl_3$/Al-PLC	1.99	187.23
Regenerated $InCl_3$/Al-PLC	1.92	176.77

After the Friedel-Crafts acylation reaction, the catalyst was filtered out of the reaction mixture, washed with ethyl acetate, and calcined at 450 °C for 4 h. In the XRD pattern of regenerated $InCl_3$/Al-PLC shown in Fig. 4.8, the broad (001) peak appeared at the same range (2θ of 4° - 8°) as that of fresh $InCl_3$/Al-PLC, indicating that the structure of catalyst was preserved upon regeneration process. Although the highest point of d_{001} was around 15.25 Å that was smaller than the d_{001} of fresh

$InCl_3$/Al-PLC. The collapse resulted from the re-calcination process and the local heat produced from decomposition of trapped organic species. The indium contents of regenerated $InCl_3$/Al-PLC and $InCl_3$/Al-PLC were slightly different, which indicates little loss of indium trichloride during catalytic reaction and regeneration process. The small amount of indium trichloride might be the $InCl_3$ particles impregnated on the outer surface of clay which could be detached easily and dissolved during the reaction. The indium chloride content and BET specific surface area of regenerated $InCl_3$/Al-PLC are shown in Table 4.10. The BET specific surface area of regenerated $InCl_3$/Al-PLC was lower than the $InCl_3$/Al-PLC. There are two reasons; (i) the re-calcination process at 450 °C was not enough to remove all organic residues that could block the pores of the catalyst and (ii) the collapse of the d-spacing also caused the smaller pores.

4.8.2 Activity of regenerated $InCl_3$/Al-PLC in Friedel-Crafts acylation of anisole with benzoyl chloride

For industrial economy, it is important to investigate the catalytic efficiency of reused catalyst. The regenerated $InCl_3$/Al-PLC was used as a catalyst in Friedel-Crafts acylation of anisole with benzoyl chloride. The results are presented in Table 4.11.

Table 4.11 Activity of regenerated $InCl_3$/Al-PLC

Entry	Catalysts	% Yield[a]
1	$InCl_3$/Al-PLC	91
2	Regenerated $InCl_3$/Al-PLC	72

[a] The yield was quantified by ^{1}H-NMR using toluene as an internal standard.

The catalytic activity of regenerated $InCl_3$/Al-PLC in Friedel-Crafts acylation is shown in Table 4.11. The regenerated $InCl_3$/Al-PLC exhibited lower activity than $InCl_3$/Al-PLC, corresponding to the result of the collapse of d_{001} spacing and lower BET specific surface area.

CHAPTER V

CONCLUSION

Aluminium oxide-pillared clay (Al-PLC) was synthesized by intercalation method, followed by calcination at 500°C for 1 h, and $InCl_3$-impregnated aluminium oxide-pillared clay ($InCl_3$/Al-PLC) was synthesized by the impregnation method of $InCl_3$ on Al-PLC, followed by calcination at 450°C for 4 h. The d_{001} spacing of Al-PLC and $InCl_3$/Al-PLC were 17.51 and 16.54 Å respectively, and the layered characteristics of clay starting materials still remained. The N_2 adsorption-desorption isotherms of both Al-PLC and $InCl_3$/Al-PLC revealed the type IV isotherm, indicating their micro-mesoporous structure. The BET specific surface area of Al-PLC and $InCl_3$/Al-PLC were higher than montmorillonite. The indium chloride content in $InCl_3$/Al-PLC was 1.99 wt%, measuring by ICP-OES.

The catalytic activities of $InCl_3$/Al-PLC were performed for Friedel-Crafts acylation of anisole with benzoyl chloride, against the activities of Al-PLC and montmorillonite. $InCl_3$/Al-PLC showed the best activity among the three. The optimized condition was using the mole ratio of anisole to benzoyl chloride of 1:3 and $InCl_3$/Al-PLC catalyst with the equivalent of 0.03 mmol $InCl_3$ in 1,4-dioxane under refluxing for 4 h. The excellent yield of 4-methoxybenzophenone (91% yield) was achieved.

The optimized conditions were also applied for the variation of both aromatic compounds and acid chlorides substrates. From the variation of aromatic compounds such as 1,3-dimethoxybenzene (84% yield), toluene (56% yield) and benzene (27% yield), yields of aromatic ketones depend on the electronic effect of starting aromatic compounds. From the variation of acid chlorides such as 4-ethylbenzoyl chloride (83% yield), butyryl chloride (87% yield) and acetyl chloride (89% yield), the type of acid chlorides does not affect the yield.

Suggestion for further work

1. Other types of pillared oxides such as iron oxide pillared clay should be used to prepare $InCl_3$-impregnated catalyst in order to investigate the combined effect of the catalysis by Lewis acid.

2. More aromatic compounds and acid chlorides should be tested to expand the scope of Friedel-Crafts acylation.

ศูนย์วิทยทรัพยากร
จุฬาลงกรณ์มหาวิทยาลัย

REFERENCES

[1] Gauthier, C., Chiche, B., Finiels, A., Geneste, P. Influence of acidity in Friedel-Crafts acylation catalyzed by zeolites. *Journal of Molecular Catalysis* 50(1989): 219-229.

[2] Yadav, G. D., Asthana, N. S., Kamble, V. S. Cesium-substituted dodecatungstophosphoric acid on K-10 clay for benzoylation of anisole with benzoyl chloride. *Journal of Catalysis* 217(2003): 88-99.

[3] Mizuno, N., Misono, M. Heterogeneous catalysis. *Chemistry Review* 98(1998): 199.

[4] Cornelis, A., Gerstmans, A., Laszlo, P., Mathy, A., Zieba, I. Friedel-Crafts acylations with modified clays as catalysts. *Catalysis Letters* 6(1990): 103-110.

[5] Quaschning, V., Deutsch, J., Druska, P., Niclas, H.-J., Kemnitz, E. Properties of modified zirconia used as Friedel-Crafts-acylation catalysts. *Journal of Catalysis* 177(1998): 164-174.

[6] Bing, Y.; Zong-shi, L., Wei-hong, Q., Gui-ru, W., Lu-bai, C. Benzoylation of anisole by benzoyl chloride over zeolite catalysts. *The Proceedings of the 3rd International Conference on Functional Molecules* 12(2005): 1-5.

[7] Yadav, G. D., Badure O. V. Selective acylation of 1,3-dibenzyloxybenzene to 3,5-dibenzyloxyacetophenone over cesium modified dodecatungstophosphoricacid (DTP) on clay. *Applied Catalysis A: General* 348(2008): 16-25.

[8] Choudhary, V. R., Jana, S. K., Kiran, B. P. Highly active Si-MCM-41-supported Ga_2O_3 and In_2O_3 catalysts for Friedel-Crafts-type benzylation and acylation reaction in the presence or absence of moisture. *Journal of Catalysis* 192(2000): 257-261.

[9] Choudhary, V. R., Jana, S. K. Benzoylation of benzene and substituted benzenes by benzoyl chloride over In_2O_3/Si-MCM-41 catalyst. *Journal of Molecular Catalysis A:* Chemical 184(2002): 247-255.

[10] Choudhary, V. R., Jana, S. K., Patil, N. S., Bhargava, S. K. Friedel-Crafts type benzylation and benzoylation of aromatic compounds over Hβ zeolite modified by oxides or chlorides of gallium and indium. *Microporous and Mesoporous Materials* 57(2003): 21-35.

[11] Choudhary, V. R., Jana, S. K., Kiran, B. P. Highly active and moisture-insensitive solid catalysts - $GaCl_3$ and $InCl_3$ supported on montmorillonite-K10 and Si-MCM-41 for benzylation of benzene. *Catalysis Letters* 64(2000): 223-226.

[12] Choudhary, V. R., Jana, S. K., Patil, N. S. Acylation of benzene over clay and mesoporous Si-MCM-41 supported $InCl_3$, $GaCl_3$ and $ZnCl_2$ catalysts. *Catalysis Letters* 76(2001): 3-4.

[13] Choudhary, V. R., Jana, S. K., Patil, N. S. Acylation of aromatic compounds using moisture insensitive $InCl_3$ impregnated mesoporous Si-MCM-41 catalyst. *Tetrahedron Letters* 43(2002): 1105-1107.

[14] Selvin, R., Sivasankar, B., Rengaraj, K. Kinetic studies on Friedel-Crafts acylation of anisole by clayzic. *Reaction Kinetics and Catalysis Letters* 67(1999): 319-324.

[15] Bruce, W. D., O' Hare, D. *Inorganic Material* 2nd ed. New York: John Wiley & Sons, 1997.

[16] Shichi, T., Takagi, K. Clay minerals as photochemical reaction fields. *Journal of Photochemistry and Photobiology C* 113(2000): 1430-1431.

[17] Moore, D. M., Reynolds, Jr. R. C. *X-Ray Diffraction and the Identification and Analysis of Clay Minerals*. New York: Oxford University Press, 1989.

[18] The structure of clay minerals [Online]. 2008. Available from: http://claymin.geoscienceworld.org/content/vol44/issue2/images/large/01-flo-01.jpeg. [2009, July 12]

[19] Michael, R., Grace, S. T., Vishnu, K. The many way of making anionic clays. *Proceeding of the Indian Academy of Science* 113(2001): 671.

[20] Jean, F. L., Georges, P. Acidity in pillared clays: origin and catalytic manifestations. *Topics in Catalysis 4* 43(1997): 34-46.

[21] Rajender, S. V. Clay and clay-supported reagents in organic synthesis. *Tetrahedron* 58(2002): 1236-1237.

[22] Tsunashima, A., Brindley, G. W., Bastovanov, M. Adsorption of uranium from solutions by montmorillonite; compositions and properties of uranyl montmorillonite. *Clays and clay minerals* 29(1981): 10-16.

[23] Shimizu, K. I., Masato, M., Kan-no, T., Hatamachi, T., Kodama, T., Kitayama, Y. Michael reaction of β- ketoesters with vinyl ketones by iron (III)-exchanged Fluorotetrasilicic mica: catalytic and spectroscopic studies. *Journal of Catalysis* 229(2005): 470-479.

[24] Shimizu, K. I., Higuchi, T., Takasugi, E., Hatamachi, T., Kodama, T., Satsuma, A. Characterization of Lewis acidity of cation-exchanged montmorillonite K-10 clay as effective heterogeneous catalyst for acetylation of alcohol. *Journal of Molecular Catalysis A: Chemical* 284(2008): 89-90.

[25] Sawangkam, P. Synthesis of tungsten containing MCM-41 catalyst and their activity for Olefin metathesis. Master's Thesis, Department of Chemistry Faculty of Science Chulalongkorn University, 2005.

[26] Diffraction of X-ray by regular planes of atoms [Online]. 2009. Available from: http://www.teachnet.ie/dkeenahan/page21.html. [2009, October 15]

[27] Donohue, M. D., Aranovich, G. L. Classification of Gibbs adsorption isotherms. *Advances in Colloid and Interface Science* 138(1998): 76-77.

[28] Analysis Software User's Manual. BELSORP, BEL JAPAN, 57.

[29] Inductively coupled plasma atomic emission spectroscopy [Online]. 2009. Available from: http://en.wikipedia.org/wiki/Inductively coupled plasma atomic emission spectroscopy. [2009, September 12]

[30] Manning, T. J., Grow, R. W. Inductively coupled plasma-atomic emission spectrometry. *The Chemical Educator* 2(1997): 7.

[31] Kanjanaboonmalert, T. Synthesis and catalytic activity in alkylation reaction of iron and gallium-dopes iron oxides pillared clays. Master's Thesis, Department of Chemistry, Faculty of Science, Chulalongkorn University, 2004.

[32] Kaloidas, V., Koufopanos, C. A., Gangas, N. H., Papayannakos, N. G. Scale-up studies for the preparation of pillared layered clays at 1 kg per batch level. *Microporous Materials* 5(1995): 97-106.

[33] Masaleh, M. Catalytic cracking of polypropylene and polyethylene using zirconium/aluminium oxide-pillared clay. Master's Thesis, Department of Chemistry, Faculty of Science, Chulalongkorn University, 2008.

[34] Kameshima, Y., Yoshizawa, A., Nakajima, A., Okada, K. Solid acidities of SiO_2-TiO_2/montmorillonite composites synthesized under different pH conditions. *Applied Clay Science* 46(2009): 183.

[35] Olejnik, S., Posner, A. M., Quirk, J. P. Swelling of montmorillonite in polar organic liquids. *Clays and Clay Minerals* 22(1974): 363.

[36] Wang, M., Muhammed, M. Novel synthesis of Al_{13}-cluster based alumina. *Nanostructured Materials* 11(1999): 1219-1229.

[37] Hart, M. P., Brown, D. R. Surface acidities and catalytic activities of acid-activated clays. *Journal of Molecular Catalysis A: Chemical* 212(2004): 315-321.

[38] Polarity of solvent [Online]. 2010. Available from: http://usm.maine.edu/~newton/Chy251_253/Lectures/Solvents/Solvents.html. [2010, April 23]

[39] Trikittiwong, P. Epoxide ring opening catalyzed by iron oxide-pillared clay. Master's Thesis, Department of Chemistry, Faculty of Science, Chulalongkorn University, 2005.

ศูนย์วิทยทรัพยากร
จุฬาลงกรณ์มหาวิทยาลัย

Appendices

ศูนย์วิทยทรัพยากร
จุฬาลงกรณ์มหาวิทยาลัย

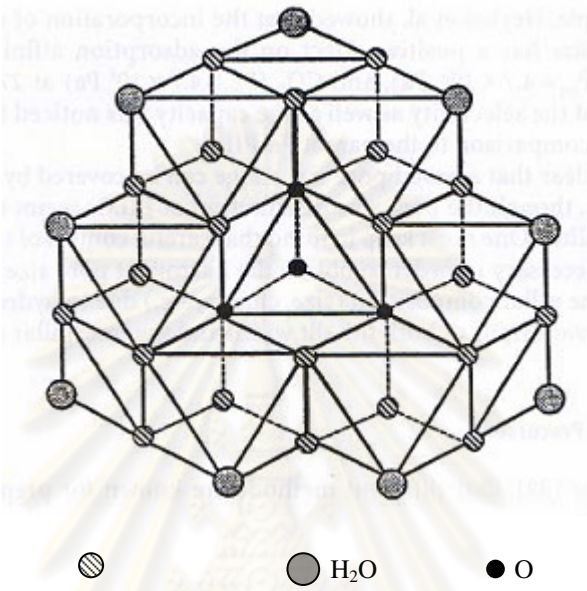

Figure A-1 Keggin structure of aluminium polyoxocation (Al_{13}).

The structure consists of one central AlO_4 tetrahedron surrounded by twelve aluminum hydroxide octahedral.

ศูนย์วิทยทรัพยากร
จุฬาลงกรณ์มหาวิทยาลัย

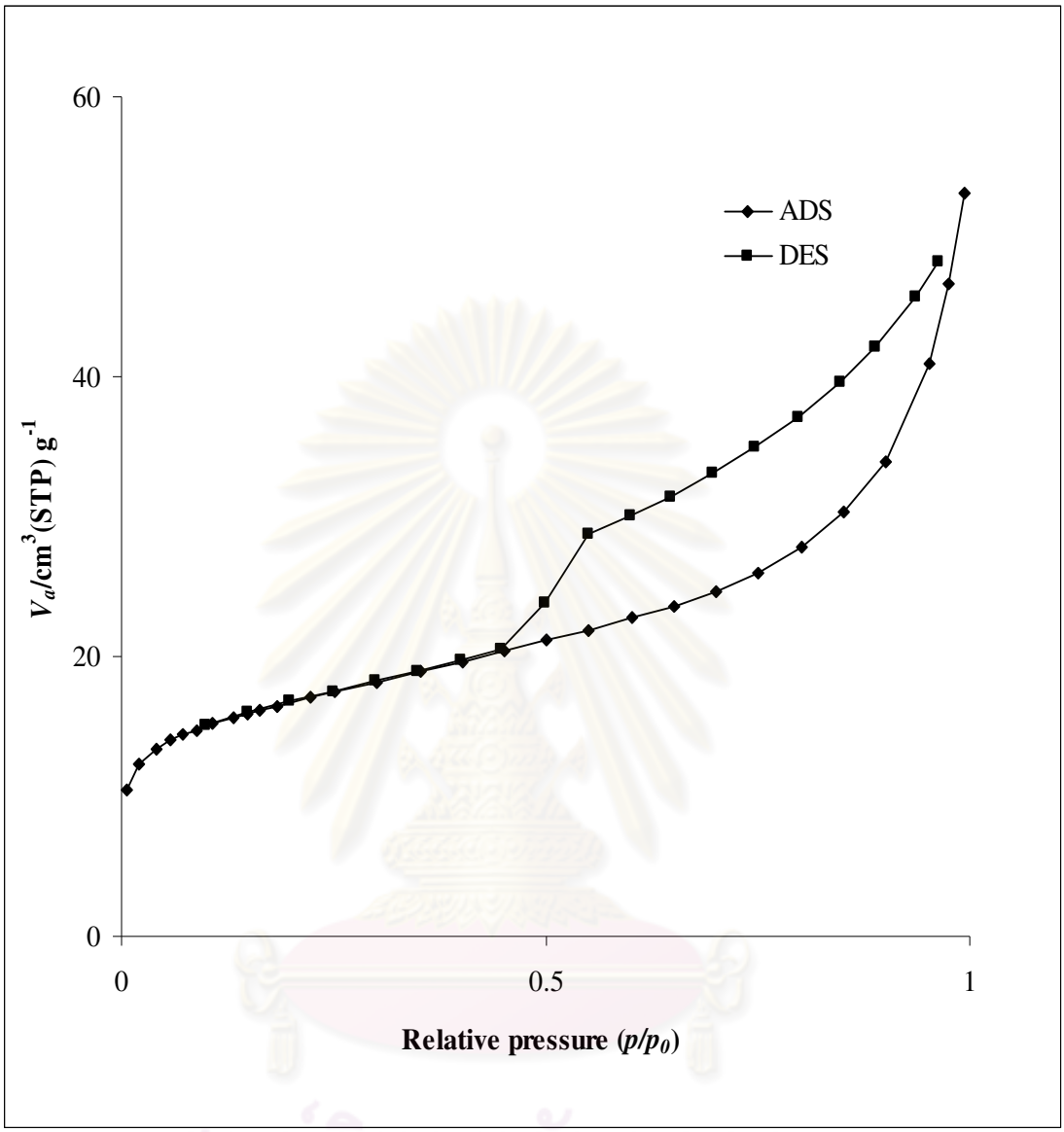

Figure A-2 N_2 adsorption-desorption isotherm of raw bentonite.

ศูนย์วิทยทรัพยากร
จุฬาลงกรณ์มหาวิทยาลัย

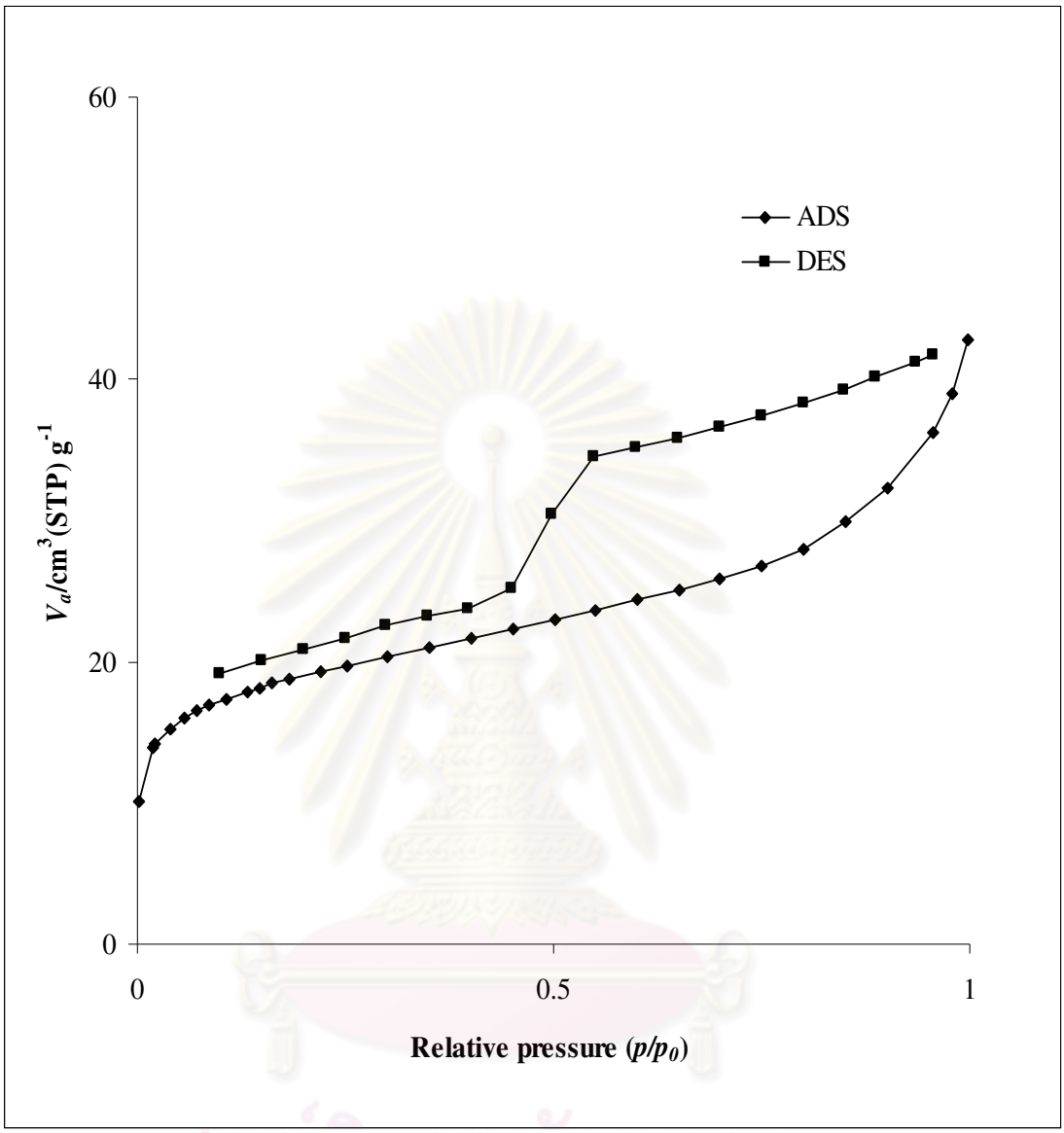

Figure A-3 N_2 adsorption-desorption isotherm of montmorillonite.

ศูนย์วิทยทรัพยากร
จุฬาลงกรณ์มหาวิทยาลัย

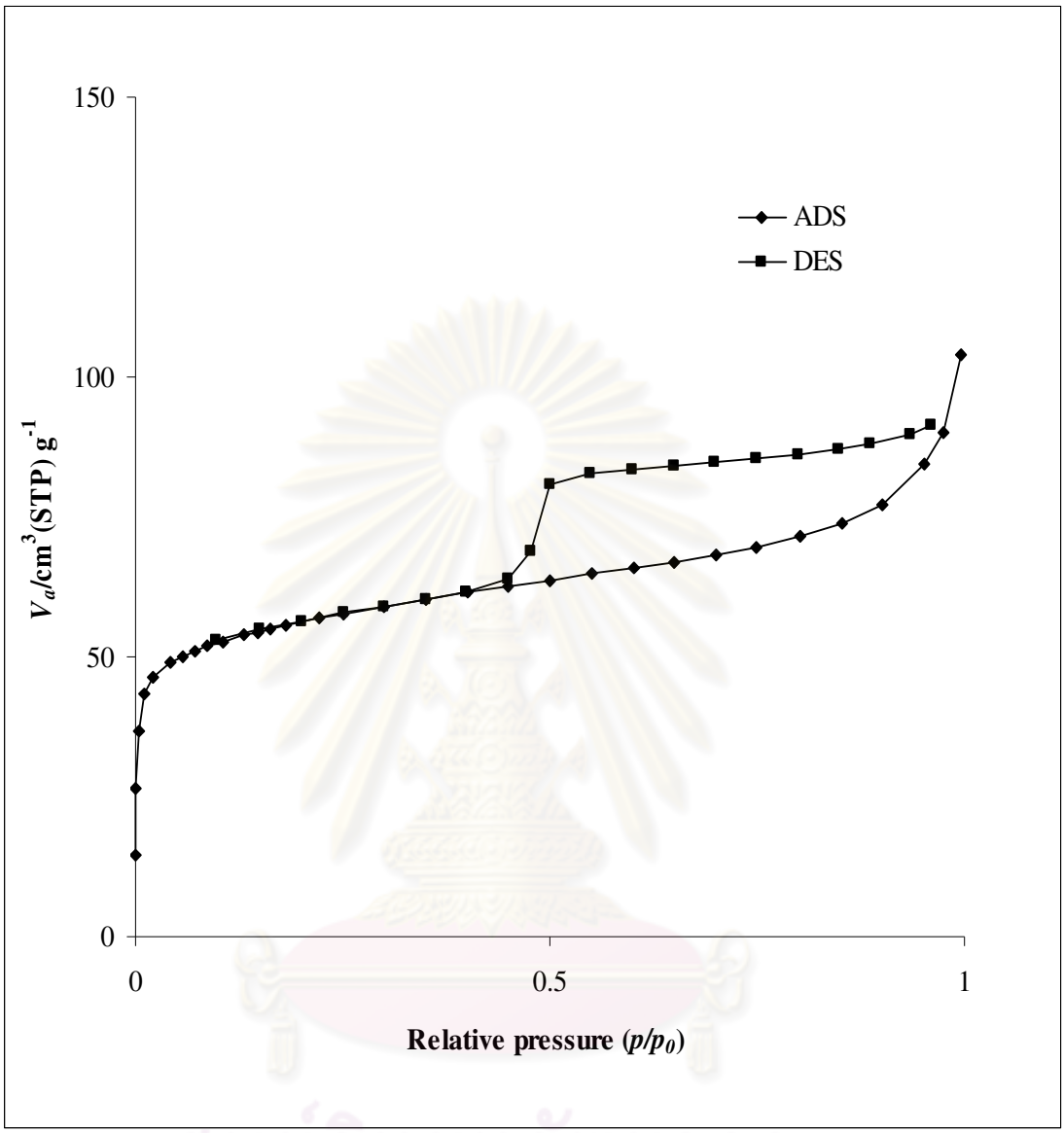

Figure A-4 N_2 adsorption-desorption isotherm of Al-PLC.

ศูนย์วิทยทรัพยากร
จุฬาลงกรณ์มหาวิทยาลัย

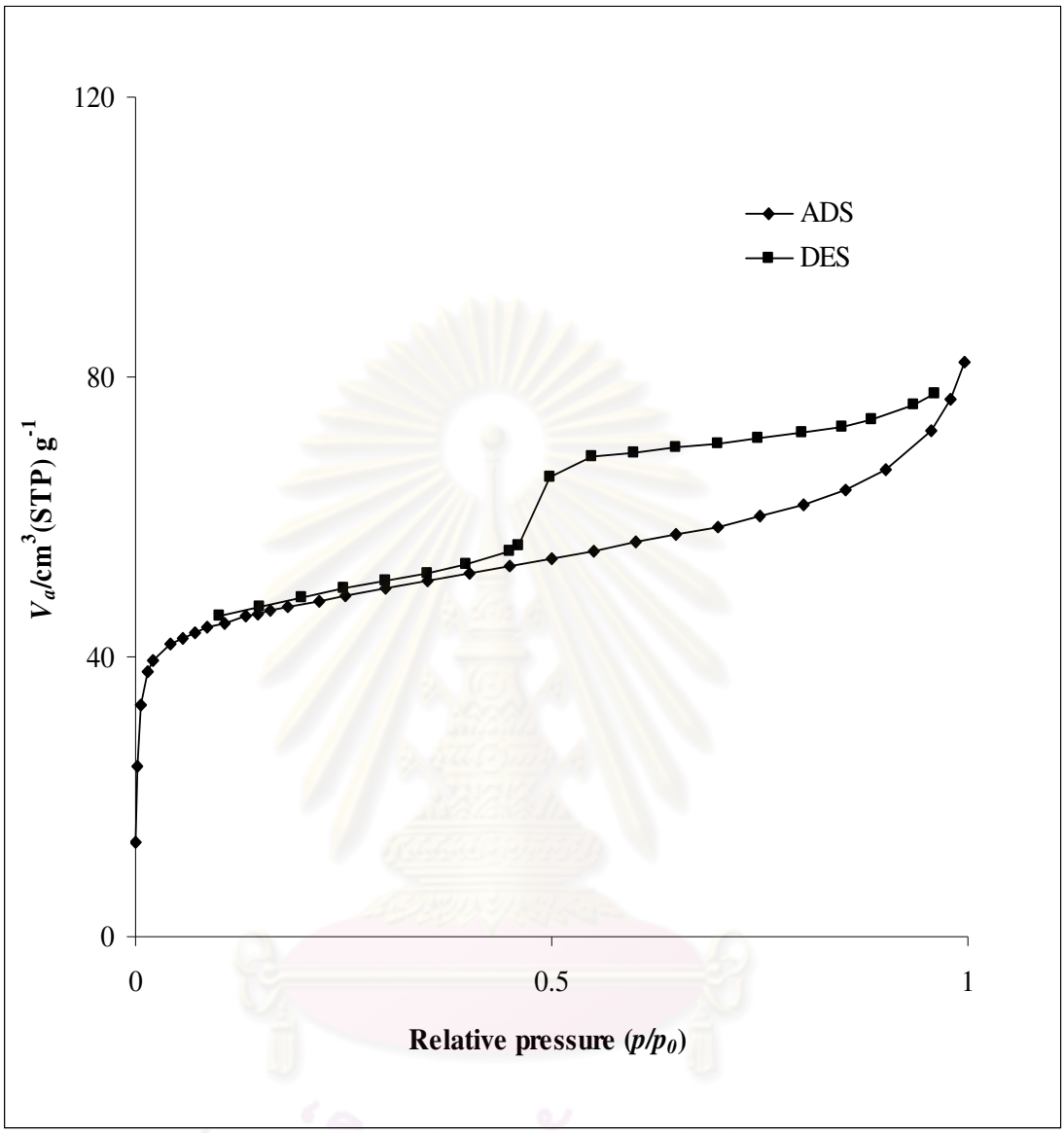

Figure A-5 N_2 adsorption-desorption isotherm of $InCl_3$/Al-PLC.

ศูนย์วิทยทรัพยากร
จุฬาลงกรณ์มหาวิทยาลัย

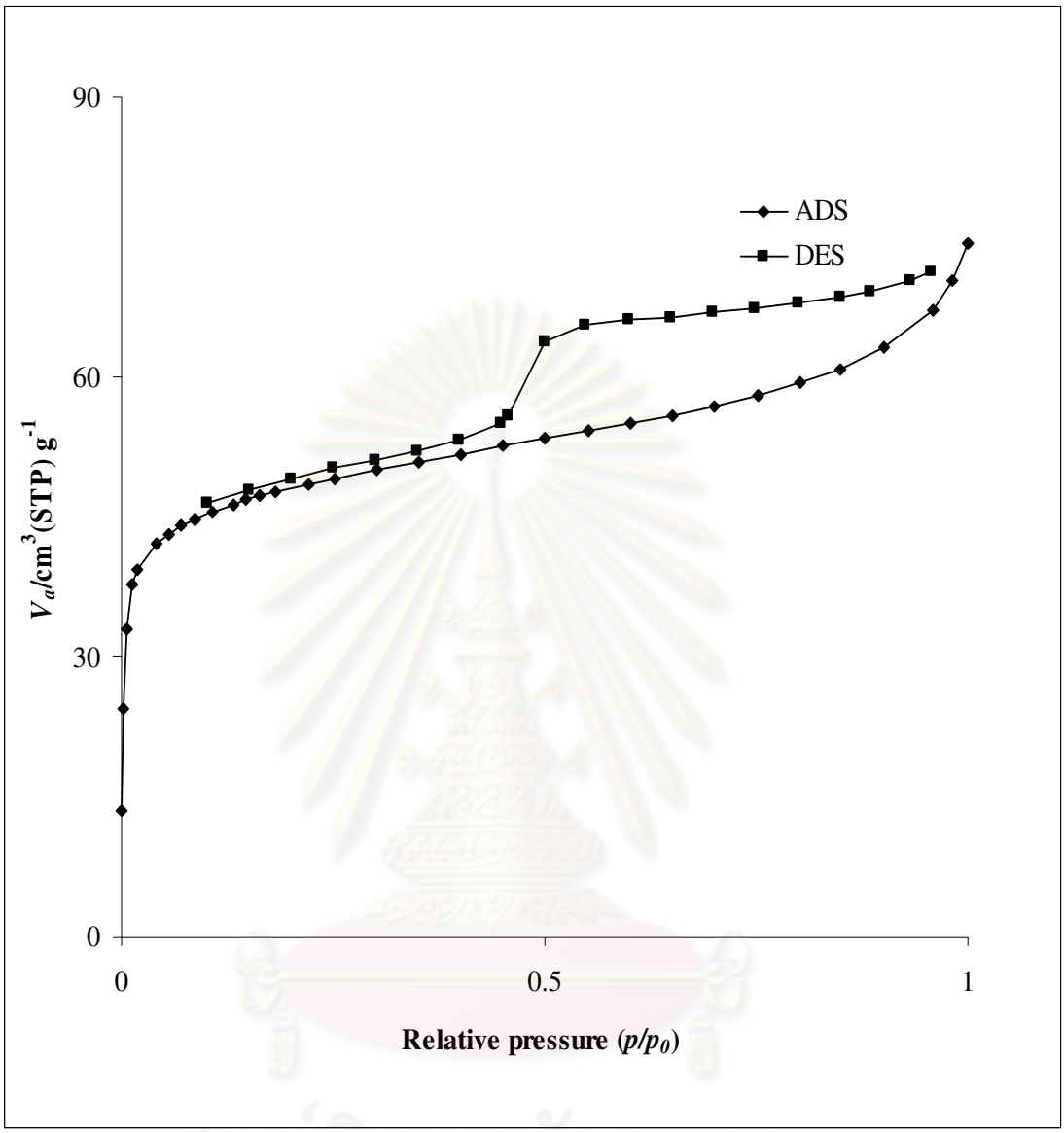

Figure A-6 N_2 adsorption-desorption isotherm of regenerated $InCl_3$/Al-PLC.

ศูนย์วิทยทรัพยากร
จุฬาลงกรณ์มหาวิทยาลัย

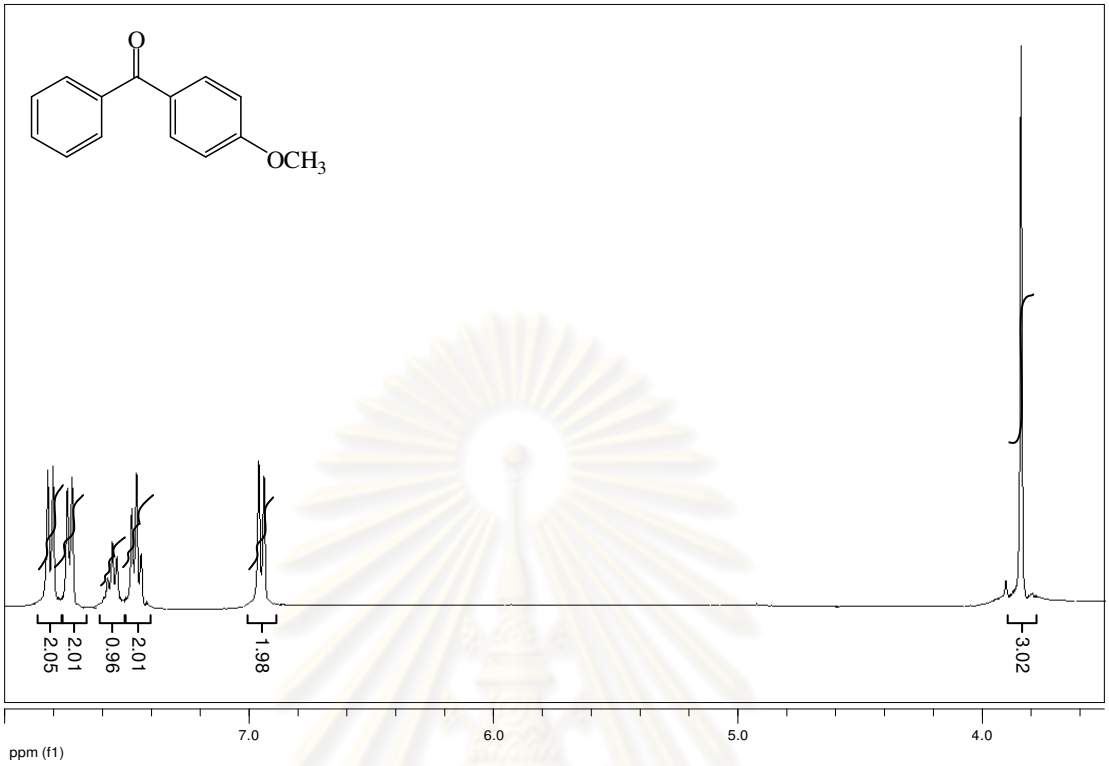

Figure A-7 The ^{1}H-NMR spectrum of 4-methoxybenzophenone.

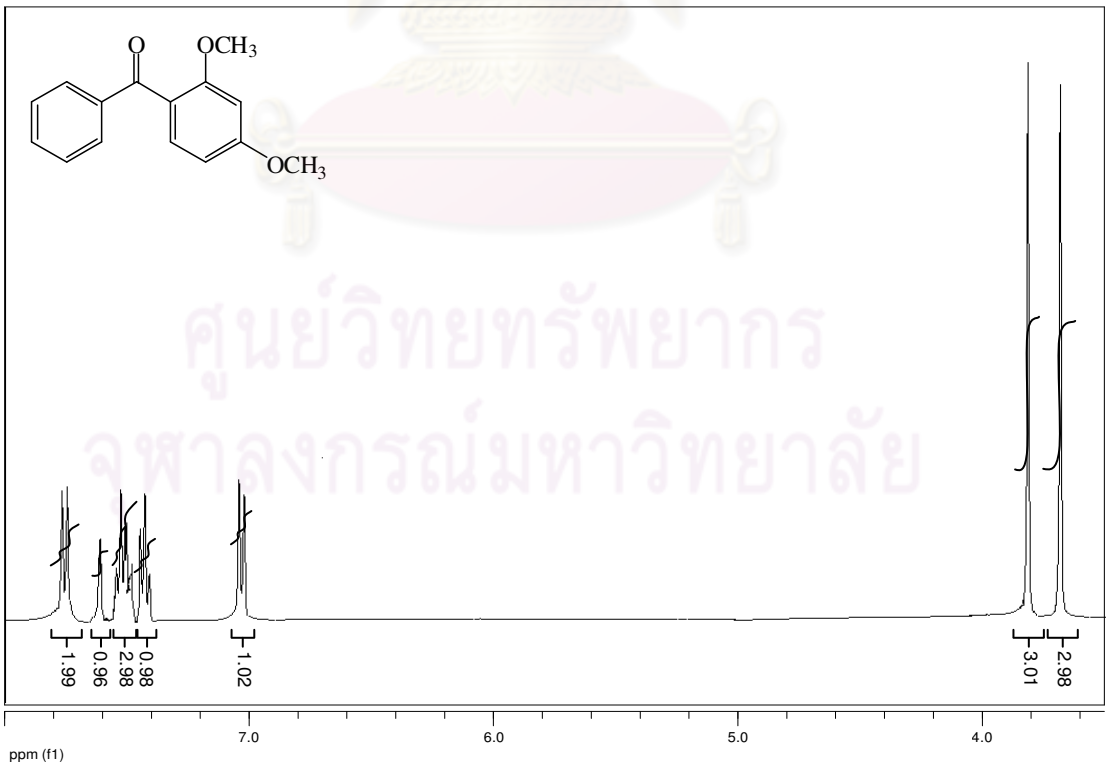

Figure A-8 The ^{1}H-NMR spectrum of 2,4-dimethoxybenzophenone.

ศูนย์วิทยทรัพยากร
จุฬาลงกรณ์มหาวิทยาลัย

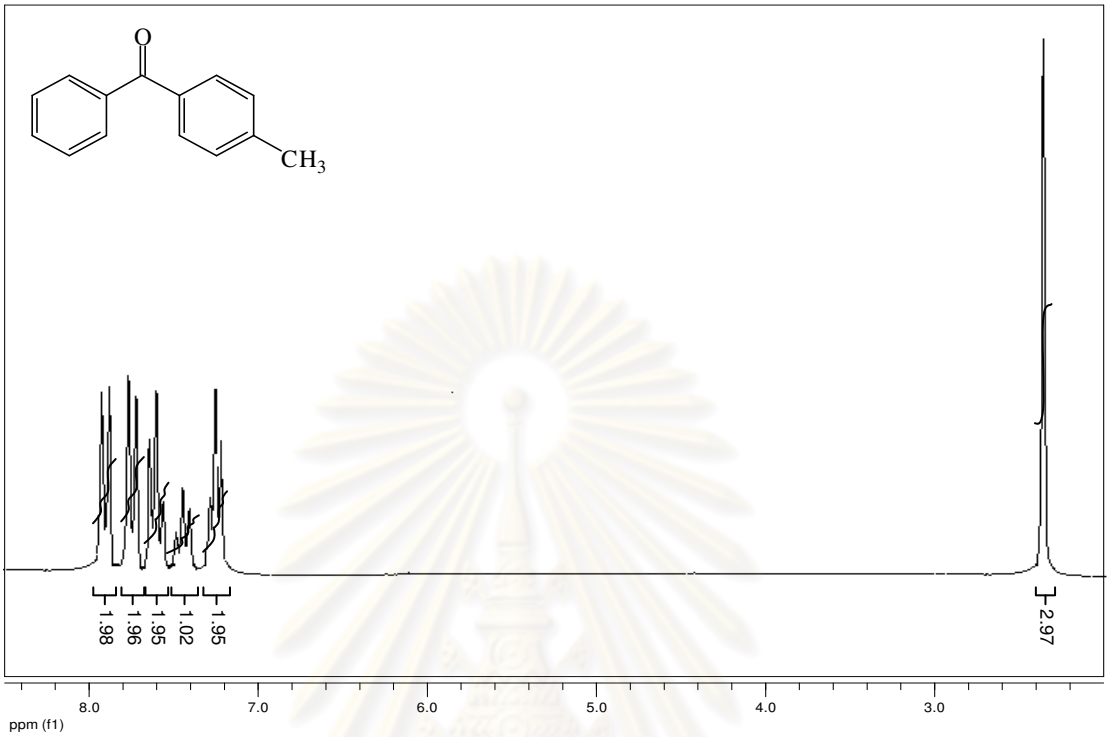

Figure A-9 The [1]H-NMR spectrum of 4-methylbenzophenone.

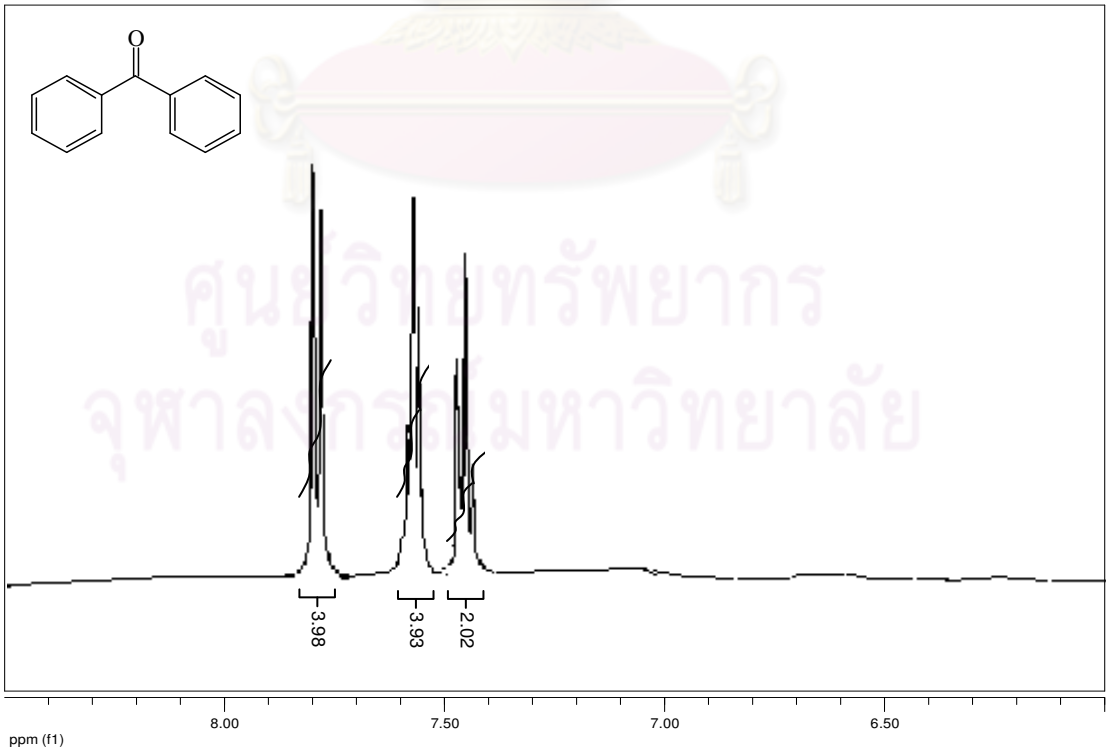

Figure A-10 The [1]H-NMR spectrum of benzophenone.

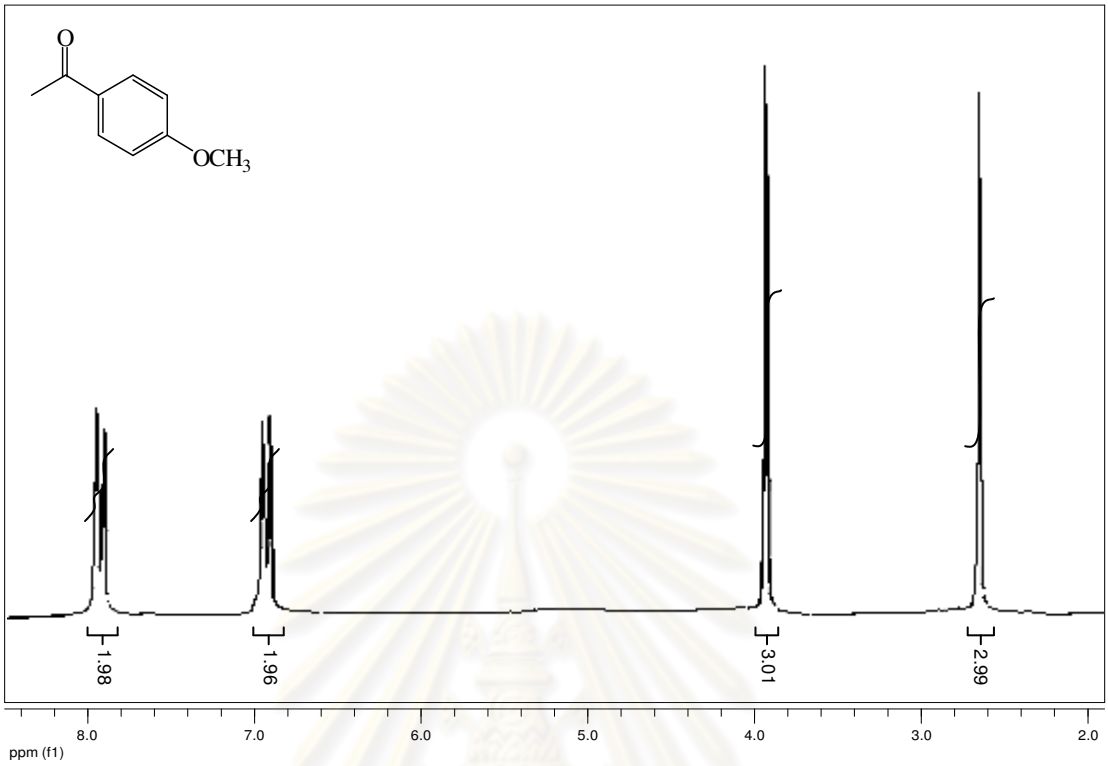

Figure A-11 The ^{1}H-NMR spectrum of 4-methoxyacetophenone.

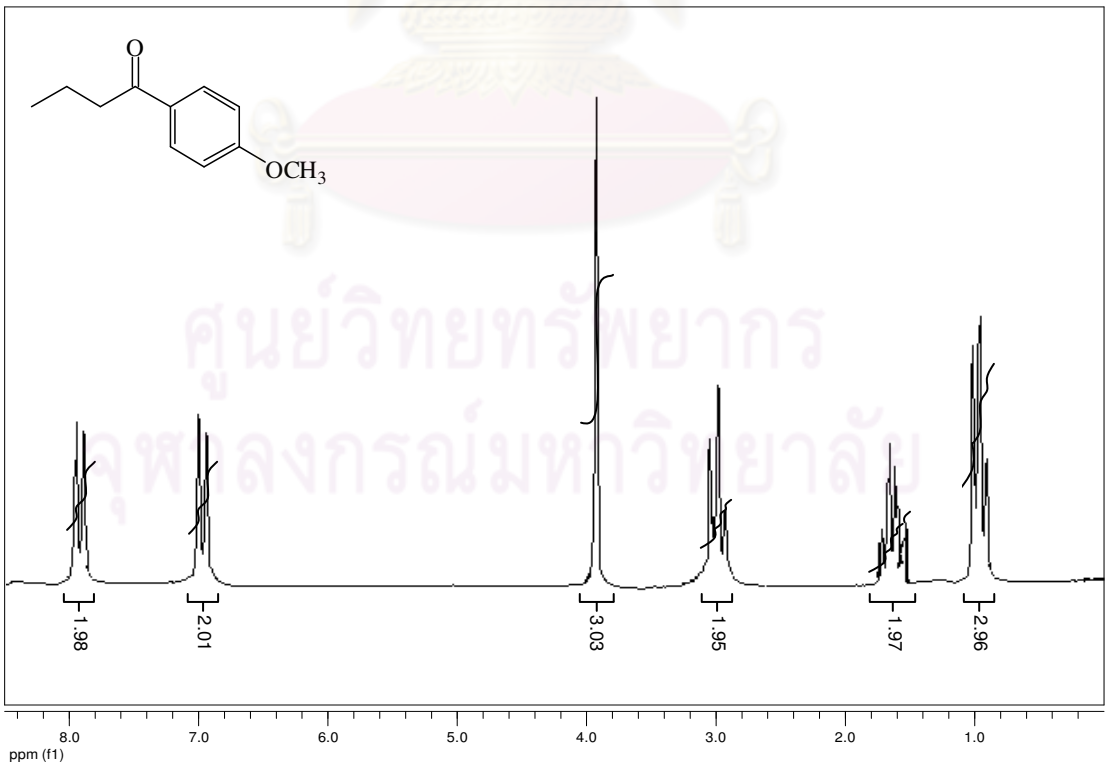

Figure A-12 The ^{1}H-NMR spectrum of 4-methoxybutyrophenone.

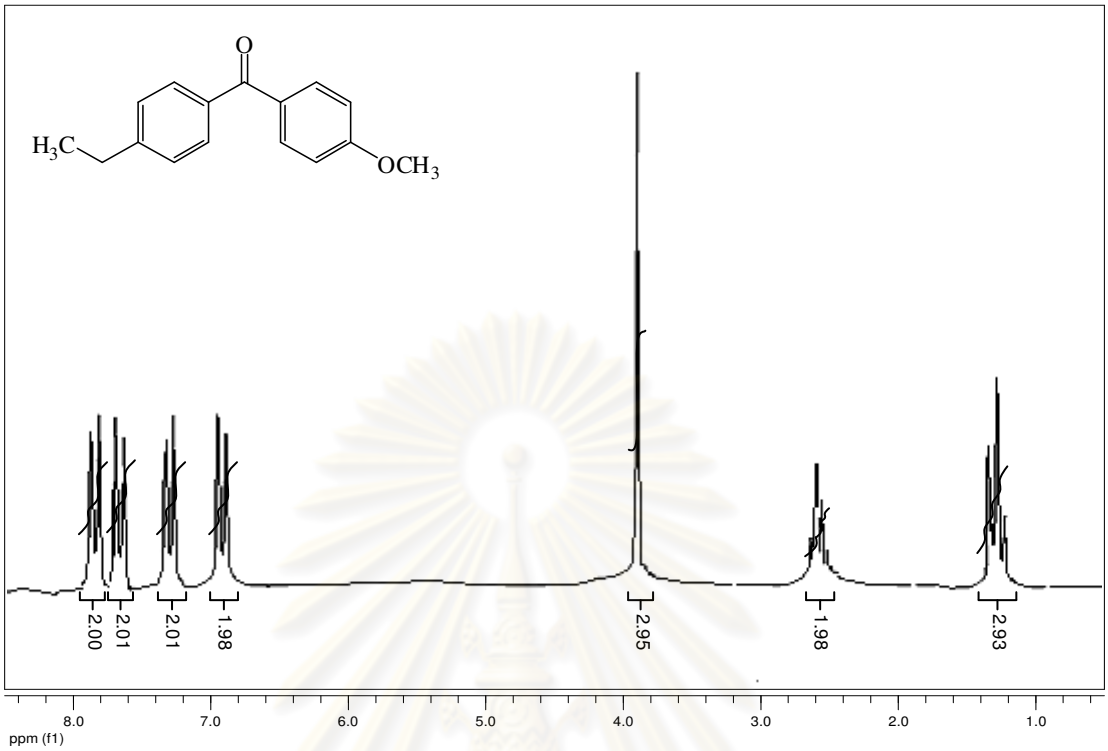

Figure A-13 The ^{1}H-NMR spectrum of 4-ethyl,(4-methoxybenzophenone).

ศูนย์วิทยทรัพยากร
จุฬาลงกรณ์มหาวิทยาลัย

VITAE

Miss Autumporn Lertwilai was born on March 21, 1985 in Samutprakarn, Thailand. She graduated from King Mongkut's University of Technology Thonburi in 2006 with Bachelor Degree of Science in Chemistry. She continued her study in program of Petrochemistry and Polymer Science, Faculty of Science, Chulalongkorn University in 2007 and completed in 2010.

Presentation

21-23 November 2009

Poster presentation "Friedel-Crafts Acylation of Anisole with Benzoyl Chloride over $InCl_3$-Impregnated Aluminium Oxide-Pillared Clay" The 6^{th} International Symposium on Advanced Material in Asia Pacific Rims, Chulalongkorn University, Bangkok.

Her present address is 100/96 M.10 Srinakarin Rd., Bangmuang, Muang, Samutprakarn, Thailand 10270. Tel: 0-86708-7673, E-mail: jibji@hotmail.com.

ศูนย์วิทยทรัพยากร
จุฬาลงกรณ์มหาวิทยาลัย